Ghahfarokhi, Payam Shams; Podgornovs, Andrejs; Kallaste, Ants; Marques Cardoso, Antonio J.; Belahcen, Anouar; Vaimann, Toomas

The Oil Spray Cooling System of Automotive Traction Motors: The State of the Art

Published in:
IEEE Transactions on Transportation Electrification

DOI:
10.1109/TTE.2022.3189596

Published: 01/03/2023

Document Version
Peer-reviewed accepted author manuscript, also known as Final accepted manuscript or Post-print

Please cite the original version:
Ghahfarokhi, P. S., Podgornovs, A., Kallaste, A., Marques Cardoso, A. J., Belahcen, A., & Vaimann, T. (2023). The Oil Spray Cooling System of Automotive Traction Motors: The State of the Art. *IEEE Transactions on Transportation Electrification*, *9*(1), 428-451. https://doi.org/10.1109/TTE.2022.3189596

The Oil Spray Cooling System of Automotive Traction Motors: The State of the Art

Payam Shams Ghahfarokhi[a,b,c], Andrejs Podgornovs[a], Ants Kallaste[b], Antonio J. Marques Cardoso[c], Anouar Belahcen[b,d], Toomas Vaimann[b]

[a]Dep. Electrical Machines and Apparatus, Riga Technical University, Kaļķu iela 1, Riga, Latvia,

[b]Dept. Electrical Power Engineering and Mechatronics, Tallinn University of Technology, Tallinn, Estonia;

[c]CISE - Electromechatronic Systems Research Centre, University of Beira Interior, Portugal

[d]Dept. Electrical Engineering and Automation, Aalto University, Finland

Corresponding author: Payam Shams Ghahfarokhi

E-Mail: payam.shams@taltech.ee

This paper has not been presented at any conference, and it has not been submitted elsewhere.

This work has been supported by the European Regional Development Fund within the Activity 1.1.1.2 "Postdoctoral Research Aid" of the Specific Aid Objective 1.1.1 "To increase the research and innovative capacity of scientific institutions of Latvia and the ability to attract external financing, investing in human resources and infrastructure" of the Operational Programme "Growth and Employment" (No.1.1.1.2/VIAA/3/19/501).

Keywords

«Automotive applications», «Direct cooling», «Electrical machine», «Oil cooling», «Spray cooling», «Thermal management», «Traction motors».

Abstract: With growing interest in green technologies and sustainable transport, hybrid and pure electric powertrains are attracting a lot of attention. According to demanded metrics such as lightweight and high-power density motors, these offer clear motivation to develop advanced thermal management methods and integrate them with conventional cooling approaches. The oil spray cooling method is one of the latest cooling methodologies integrated with the conventional cooling approaches. Therefore, this article provides a comprehensive study on the oil spray cooling approach for electrical motors utilized in EV traction application drives. The objective is to provide the reader with a picture of state of the art regarding the opportunities, challenges, and offered solutions for the cooling requirements in EV motors.

Additionally, the paper presents the guidelines for selecting the appropriate spray nozzles and coolants as well as estimating their performance, spray characteristics, and heat transfer coefficient (HTC) during the design period. Besides, various closed-loop systems of spray cooling approach, including refrigerants as a coolant, low viscosity liquid coolant with high boiling temperature, and high viscosity lubricant oil as a coolant, are discussed with the pros and cons of each system being compared. Moreover, real-life examples of this method, applied in the latest automotive traction motor prototypes, have been described and evaluated. Finally, the performance of different schemes is addressed.

I. Introduction

The negative ecological footprint of combustion engines, global warming, and the sustainable energy program intended to mandatory minimize the CO_2 emissions for new cars significantly impact the research and development of electrical machines for traction application purposes. Based on the European Green Deal Roadmap, all new vehicles must have a maximum of 95 g of CO_2 emission per km, amounting to fuel consumption of around 4.1 l/100 km of petrol or 3.6 l/100 km of diesel fuel [1], [2]. Moreover, the US Department of Energy (DOE) defined the objectives to be achieved by 2025; a power density target of 33 kW per liter and a cost target of US $ 6 per kW for a 100 kW electric traction drive system [3]. To achieve these targets, the automotive industry has started to develop a new generation of cars by replacing the combustion engine with an electrical engine or by synthesizing the combustion engine and electrical engine independently or jointly, as hybrid electric vehicles [4], [5], [6].

The growing transport electrification market directly impacts the increasing current density, the peak powertrain powers, and torque density of these motors. Furthermore, the motors utilized for EV traction drive applications are incredibly compact with higher rotational speed [7]. As shown in Fig.1, for the high power density EV motor, there are limits for utilizing only the conventional cooling methods [8], for instance only cooling jackets [9], [10] or air-cooled [11], [12]. Hence, integrating the conventional cooling methods with complex in-direct or direct cooling systems is required to provide sufficient heat extraction from stator winding and rotor parts.

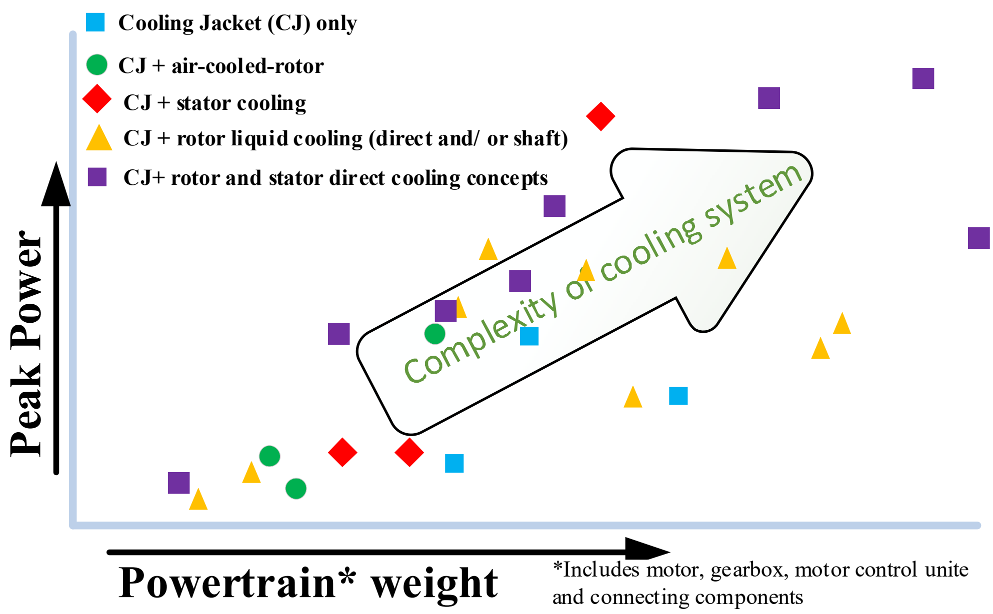

Fig. 1. Variation of the thermal management system of EV motors by increasing their peak power [8].

Table I. Overview of thermal management systems in EV motors according to EV motor evolution

Vehicle /Motor	Year	Motor Type	Cooling Methods	Peak Power (kW)	Top Motor Speed (rpm)	Ref
Toyota Prius	2010	IPMSM	Housing jacket cooling with oil	60	13500	[13]
Sonata	2011	PMSM	Housing jacket cooling with oil	30	6000	[13]
Nissan Leaf	2012	PMSM	Housing liquid (water) jacket	80	10390	[14], [15], [16]
Tesla Model S6	2013	IM	Housing liquid (water) jacket and shaft cooling	225	14800	[17]
Toyota Prius	2017	PMSM	Automatic transmission fluid (ATF) stator cooling and ATF spray cooling of end winding	53	17000	[18]
Tesla Model 3	2018	IPMSynRM	ATF rotor shaft cooling with radial winding spray cooling and stator yoke cooling channels	192	17900	[8], [19]
Porsche Taycan,	2020	PMSMs	Housing liquid jacket and direct cooling jacket	190/335	16000	[8], [20]

Table I shows the evolution of EV motors and their thermal management systems during the recent decades. In the first generations of EV motors, an in-direct liquid cooling method has been proposed to form the primary motor cooling [9], [10]. In this method, the housing liquid jacket is applied around the outer circumferential stator. Fig. 2 shows three circumferential channels in the housing of the Nissan Leaf acting as a water jacket to cool the motor.

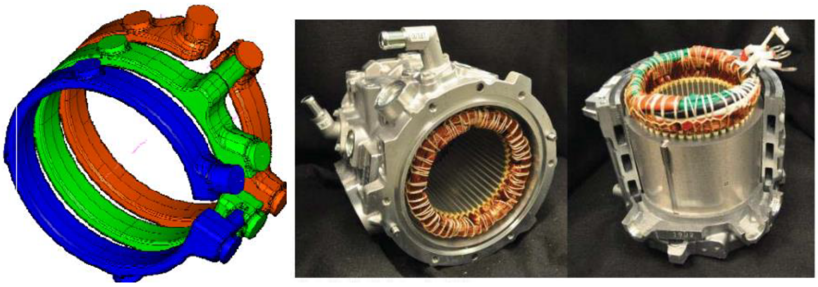

Fig. 2. Nissan Leaf motor and its water-cooling jacket [15], [16].

However, the current demanded metrics of EV motors are mainly concentrated on high power density, high efficiency, and lightweight [21], [22]. Consequently, it is impossible to achieve the mentioned demands using only housing liquid jackets. First, it increases machine diameter and housing dimensions, leading to higher EV motor volume and weight, contrary to the mentioned demanded metrics [21]. Secondly, due to the long thermal path, this cooling approach does not effectively cool the stator end windings and rotor [13], [23]-[25]. Therefore, for the next generation of EV motors, the conventional cooling methods such as housing liquid jackets are integrated into the in-direct or direct cooling systems (Fig. 3), such as, stator slot cooling [26]-[30], stator core cooling [17], [31]-[34], end winding cooling [25], [35]-[38] and rotor cooling [13], [17], [39]-[41] to sufficiently cool the critical parts of the machines.

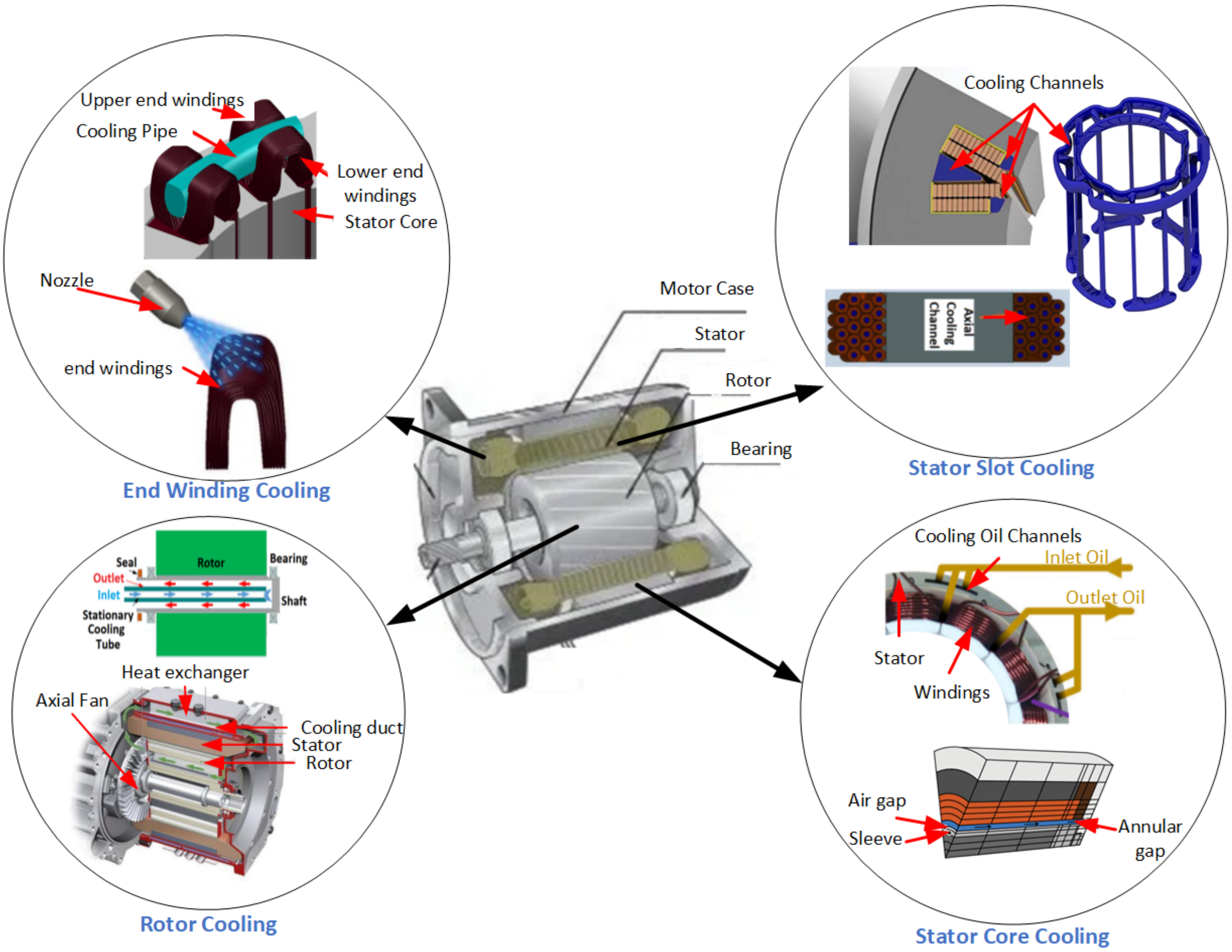

Fig. 3. Various cooling concepts for EV motors [13], [33], [35], [36].

Semi-flooded cooling, shown in Fig. 4, is one of the efficient stator cooling approaches for which the coolant (oil) is in contact with the internal parts of the electric motor and directly wet them. As EV motors are used in high-speed applications, the separating sleeve (Stator Can) is installed in the air gap to avoid the additional losses of high viscous generated heat (due to the coolant contact in the air gap with the high-speed rotor). Therefore, this sleeve separates the stator part (immerging in coolant) as a wet chamber and the rotor part as a dry chamber. Since, in this cooling approach, the coolant (oil) recirculates near the air gap, the heat transfer distance for the rotor losses to the coolant is decreased, and more efficient cooling is achieved for the rotor.

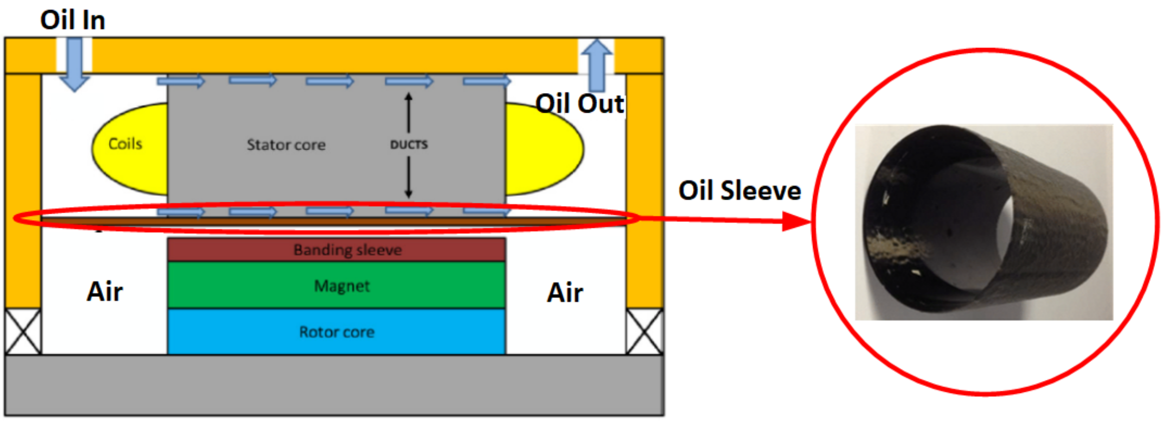

Fig. 4. Semi flooded cooling approach [31]-[33].

The most practical EV motor technologies are the interior permanent magnet synchronous motor (IPSM) and the permanent magnet assisted synchronous reluctance motor (PMASynRM). However, the increase in the price of rare earth materials and the negative environmental impacts of magnet manufacturing from rare earth materials lead the automotive industries to research and develop rare-earth-free motor technologies [42]. The essential factor in these new technologies is the motor's air gap length, which should be small as possible to save the motor performance. Therefore, these motors consist of a tiny air gap, and installing the oil sleeve in these compact motors is quite challenging [25]. Overall, due to the additional essential requirements to mitigate friction losses, short-circuit faults, and corrosion, this direct liquid cooling has no economic and practical justification [40].

Another advanced cooling approach is focused on directly or indirectly cooling the stator windings. In a direct system, shown in Fig 5, the stator winding includes the hollow solid wires or hollow copper bars to provide a water path inside the windings (internally cooled hollow wires), and the heat losses can be dissipated from the place where they arise [26], [27], [29]. Moreover, by implementing this method, the current density can be increased to more than 50 A/mm^2 [29]. However, implementing this direct liquid cooling for EV motors causes several drawbacks, such as higher cost due to better winding insulation for the material directly in contact with the coolant. Besides, this cooling system needs a high filling factor and a bigger slot size. As a result, this cooling system is mainly implemented on bus traction motors [27].

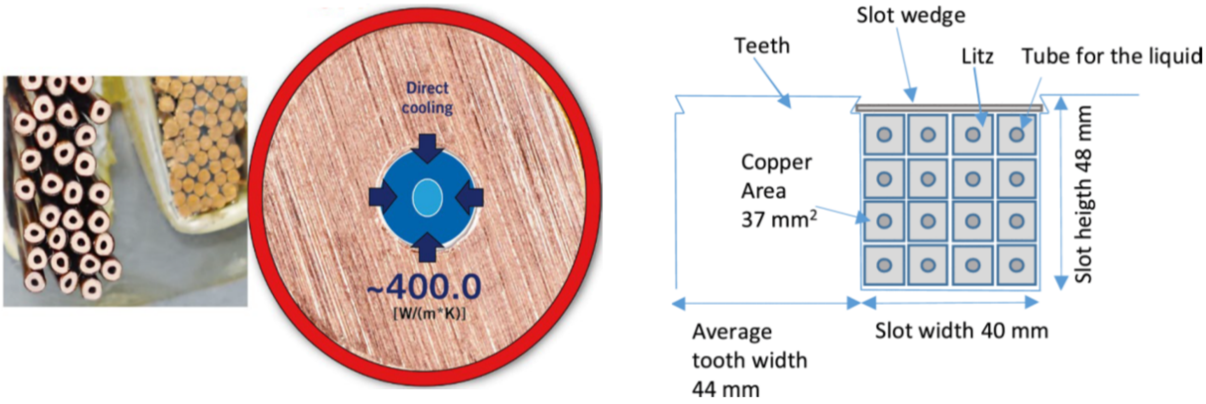

Fig. 5. Example of internally cooled hollow wires [26], [29].

In the indirect cooling method of stator slot windings, the heat exchanger is located axially inside the stator slot. The glycol-water mixture flows as a coolant in this heat exchanger [43], [44]. This cooling technology is developed as an alternative option for the semi flood oil-cooled motors to reduce the thermal management system's weight, cost, and complexity [45]. However, this technology is mainly used for motors with concentrated winding, such as switch reluctance motors.

Another thermal management concept is focused on providing good heat removal from the rotor. In motors with an internal rotor structure, the air gap acts as a thermal insulator and dramatically reduces the heat transfer from the rotor [13]. Therefore, the rotor is the first component to reach its temperature threshold [39]. Since implementing a direct cooling approach in an EV motor rotor is complex [13], the in-direct shaft cooling system is proposed to dominate the above issue. In this cooling approach, the motor shaft consists of the concentrate tubes in which the coolant (oil or water) flows back and forth. This method is implemented chiefly for EVs with induction motors such as Tesla Model S [46] and Audi e-torn [47]. Therefore, the motor performance is considerably increased, and the rotor cooling can be combined with the stator cooling system, as shown in Fig. 6. However, from the practical point of view, this is complex and can increase the motor's axial length.

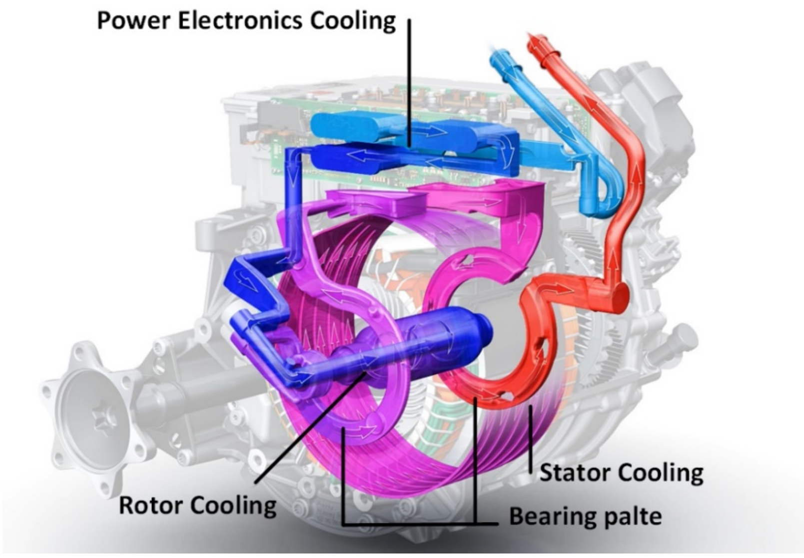

Fig. 6. Integrated rotor and stator cooling systems [47].

The latest cooling concept focuses on cooling the end windings directly (as they are identified as machine hot spots). This cooling approach is divided mainly into three different systems, semi-flood [31]-[33], dedicated liquid-carrying pipe [35], [36], and spray cooling approach [25], [38], [48], [49]. Semi flood cooling system has been analyzed briefly with its advantages and drawbacks in stator cooling approaches, and it is not considered here again.

The dedicated liquid-carrying pipe cooling technique is a direct thermal management technique to cool machine end windings uniformly by installing the pipe on the end windings. In this technique, the pipe is dividing the end windings into upper and lower sections, and by passing the liquid coolant from the pipe, the heat is extracted directly from the end windings. Besides, it enhances the axial heat transfer in the slot and reduces the slot's midsection temperature. However, this cooling technique is suitable for concentrated windings, as a new technique still under development and not practically implemented in any commercial EV motors.

Recently, electrical machines with hairpin windings are becoming a more popular and attractive solution to electrical motors for EV applications due to their numerous advantages compared to the conventional stranded winding configuration. For example, this topology provides a more straightforward manufacturing process, handling higher current density, higher slot filling factor, good thermal performance, shorter end winding, and lower DC electrical resistance, as well as lower manufacturing time and cost [25], [50]-[53]. Therefore, different automotive companies have started implementing this winding configuration on their new generation of electrical engines, such as GM-Volt-Motor and Chevrolet-Volt [52]. Moreover, the oil spray cooling approach is one of the most attractive cooling systems that perfectly match these high current density motors. For instance, the Toyota company unveiled the hairpin winding and direct oil spray cooling method in its latest Toyota Prius [18]. Therefore, Toyota decided to upgrade its Prius 2009 with motor P410 [18]. For this purpose, the company developed the new concept using hairpin windings' configuration and oil spray cooling approach and calls it P610 [18]. According to Toyota's report, the new design provides a more compact motor with higher efficiency than P410 [18]. Generally, the motor size was reduced by about 35%, with a 36% higher power density and 20% fewer losses [18]. Therefore, the combination of hairpin windings and oil spray cooling as its thermal management system attracts the attention and provides the solution to develop the new EV motors design with a more compact structure and higher power density.

The oil spray cooling approach is the direct liquid cooling trend for the next generation of EV traction motors. This cooling approach aims to cool stator end windings and rotor directly. In this approach, the liquid coolant (oil) is forced to pass through the tiny orifice to change fluid into small droplets spread on the end winding's hot surface [54]. Fig. 7 shows the spray cooling of the stator end windings and rotor, which cools by spraying oil as a liquid coolant from the spray rings.

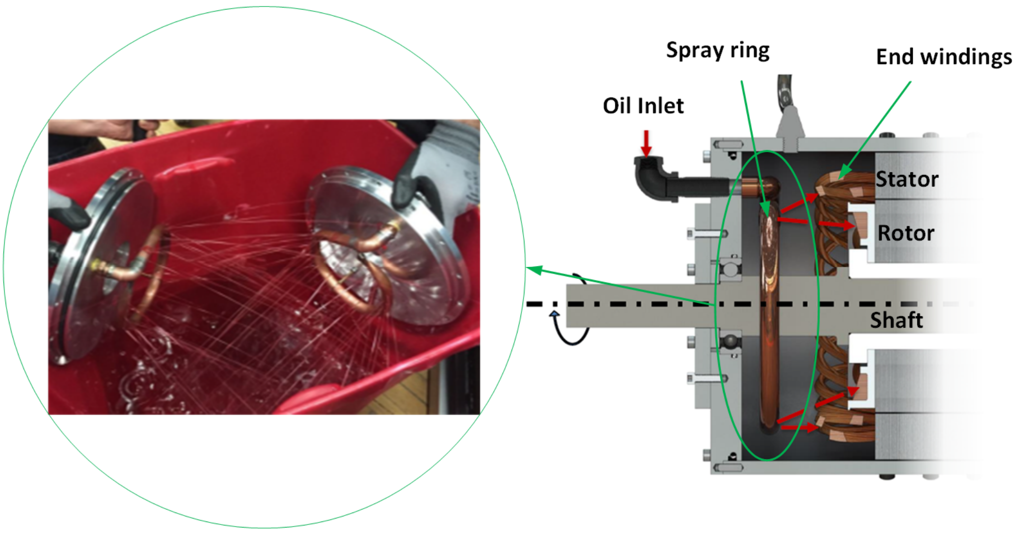

Fig. 7. Spray cooling on rotor and stator end windings [55].

This approach has significant advantages in enhancing axial heat transfer in the slot, removing enormous heat energy, and reducing the conduction path from the end windings with no extra electromagnetic fluctuating or additional electric noise [13], [48] and [54]. The performance of a motor for traction application purposes has been considered in [56] according to the following three thermal management systems: stator liquid jacket including microchannels, slot heat exchangers in the form of tubes, and end winding spray cooling. As it is reported in [56], the spray cooling approach provides the most effective cooling with less complexity and a high possibility of mass production.

The spray cooling approach is not a new technique in itself, and it has been studied over decades in various engineering and scientific fields. However, these studies showed that the spray cooling approach is used chiefly for lower-viscosity liquid coolants such as water. Therefore, there is insufficient information and data about the spray behavior and spray cooling of high-viscosity liquids, such as engine oil. Moreover, spray cooling is utilized in electronic and power electronic devices to cool small surfaces without any rotational sections to disturb oil uniformity distribution. However, unlike electronic and power electronic devices, this approach is used to cool the most complex motor part, the end windings; hence, the designers face more complex geometries and more expansive hot surfaces affected by rotor rotation. Consequently, they face more challenges, such as system complexity and the uneven temperature distribution in the end-winding region.

So far, there is no adequate information about the oil spray cooling system and its performance with high viscosity coolant, suitable nozzles, and appropriate spray patterns. Therefore, this paper provides comprehensive practical information about the right spray system for high viscosity coolants, its mechanism, and components, such as various nozzles and their performances. Then, it provides the state-of-the-art about all the attempts to utilize this thermal management system for electrical motors, analyzing the progress, advantages, and drawbacks. Finally, the paper discusses the perspectives on improving the weaknesses and drawbacks of this cooling system.

The paper is organized as follows: Section II is established by considering the spray cooling system, its mechanism, components, progress, and challenges. Section III mainly considers all the attempts using this thermal management system for electrical machines, their findings, progress, advantages, and disadvantages. Section IV presents the search for suitable empirical correlation to estimate the HTC from the end windings of the machines for various conditions. Section V discusses the perspectives of this cooling system and the improvements that must be considered. Finally, a conclusion from this research is summarized in section VI.

II. Spray Cooling System

Spray cooling is a closed-loop system with a complex structure including a coolant, tank, pump, nozzles, and cooling temperature unit. First, the pump enhances fluid pressure from the tank to the nozzle in this system. Then, the nozzle alters the liquid into tiny droplets and spreads them to the hot surfaces. Ultimately, the excess coolant in liquid or a mixture of liquid and vapor (in a two-phase system) is gathered and sent to the temperature control unit to remove the heat and prepare for recirculating.

This thermal management system faces two main challenges: system complexity and uneven temperature distribution. The system complexity mainly depends on the coolant, and uneven temperature distribution is related to the number of nozzles and their spray patterns that cannot cover the entire area equally. Consequently, the coolant and nozzle are the most crucial components in this system whose right choice may significantly improve the cooling efficiency. Several research studies have investigated the impact of these components on spray cooling and the choice of alternative coolant and nozzle for spray cooling of the current-carrying components [25], [48], [57], [58]. Therefore, at the beginning of this section, different coolants' impact on the cooling system's complexity and their evaluation over the years are investigated. Then, the right choice of the nozzle, as the primary device to generate the spray flow and enhance the system's performance, is considered in detail.

a. Coolant Selection

Due to stringent material and electrical compatibility provisions in the spray cooling system of electric devices, it is prohibited to utilize water as a coolant in direct contact with current-carrying components. Several research studies investigated the alternative coolants for spray cooling of the current-carrying components [25], [48], [49], [57]-[60]. However, most of these studies focus on the spray cooling of hybrid vehicle electronics rather than electric motors.

The proper coolant for spreading electrical components must include several different requirements, such as [57], [61]:

- Good environmental adaption;
- High safety;
- High dielectric strength;
- Good material compatibility.

From the environmental point of view, a coolant is considered by the ozone depletion potential (ODP) and the global warming potential (GWP) factors [57],[61]. From the environmental point of view, a suitable coolant must consist of zero ODP factor, and the GWP factor must be less than 1500. For an average coolant, the ODP factor is defined between zero and 0.1 (0<ODP<0.1), and GWP should be in the range of 1500 to 6000 (1500<GWP<6000) [57], [61]. Also, for safety objectives, the coolant is considered by the flammability. Thus, a suitable coolant is nonflammable, and a poor coolant is flammable [57], [61]. From a dielectric strength point of view, it is considered the possible high voltage that the coolant may tolerate without breakdown and arcing in the coolant [57], [61]. Finally, as far as the material compatibility is concerned, parameters such as the atmosphere lifetime (time needed for coolant concentration in the atmosphere to drop to *1/e* of its initial value) have to be determined [57], [61].

Selecting the appropriate coolant for spraying electronics and electrical components is challenging. As Fig. 8 shows, depending on the coolant types, the number of sub loops and devices of the control temperature unit varies significantly. There are three alternative options for the coolant: refrigerants, liquid coolants with high boiling temperatures, and lubricant oil. All three options are considered here, regarding their performance, cooling system, and advantages and drawbacks.

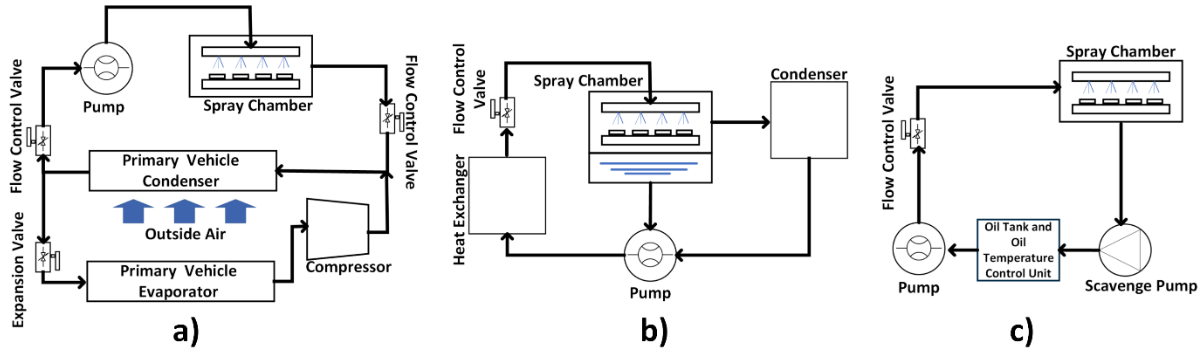

Fig. 8. Closed-loop systems for spray cooling approach: a) refrigerants as a coolant, b) low viscosity liquid coolant with high boiling temperature, and c) high viscosity lubricant oil as a coolant [57], [61], [62].

Refrigerants started to be utilized as a coolant due to the low saturation temperature and boiling point, which allowed the system to benefit from phase-change cooling. One of the first refrigerant materials was introduced as a coolant from the chlorofluorocarbon (CFC) family [57], [61]. The most famous ones are R11, R12, R113, and R114. These materials are categorized as high ozone-depleting and global warming potentials [57], [61]. Consequently, the CFC material is changed by new refrigerant material from hydrofluorocarbons (HFCs) families (such as R123, R124, and R141b) to adapt to the coolant requirement [57], [61]. This new refrigerant family provides almost similar cooling characteristics, with a 10 % lower ozone depletion than CFC [57], [61]. Recently, new HFCs (e.g., R134a and R143a) are replaced by the previous ones that benefit from zero ODP and lower global warming effects [57], [61].

The refrigerant as an evaporating coolant is pumped to the heat source in the phase-change cooling system. Then, it converts to vapor (gas coolant) by absorbing the heat energy and reaching the boiling point (after absorbing the heat energy). Next, the coolant moves toward the condenser to transform (condensed) into the liquid, and it backs to the cycle in the final part of the loop [13].

These spray cooling systems benefit from two-phase heat transfer regimes; some portions of the coolant are converted to vapor and increase the heat transfer by convection. Fig. 9 illustrates the general spray cooling curve, which shows the heat flux versus wall temperature of a flat copper heater cooled by the spray cooling method. Fig. 9 provides single-phase and two-phase heat transfer regimes for this case study. Thus, until the surface temperature is less than 70 °C, the curve is located in a single regime with a linear behavior. In this situation, the supplied liquid has a sufficient rate to replace the fresh drop of coolant. Continue with increasing the heat flux and reaching the superheat condition (more than 70 °C), it enters the two-phase regime, and the slope of the curve becomes sharper.

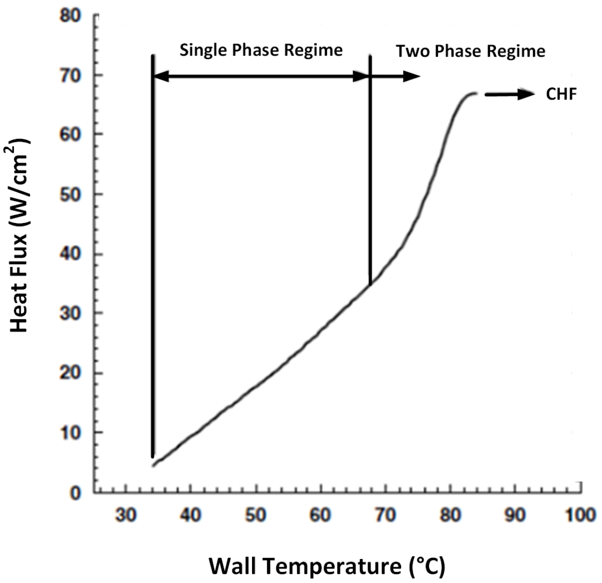

Fig. 9. Spray cooling curve of a copper heater (Coolant=FC-72, flow rate=93 ml/min, inlet pressure= 1.0 bar, T_{sat}*=57°C,*ΔT_{sub}*=28°C, Area of copper heater=2 cm*^{2}*)* [54].

The complex system structure is the drawback of the fluorocarbon family or mainly refrigerant family as a coolant. According to Fig. 8 a), the cooling loop system of refrigerant coolants consists of sub loops that cause an increase in the system's cost and complexity. Hence, the refrigerant coolants were replaced by liquid coolants with a higher boiling point to overcome the closed-loop system's complexity and greater flexibility in selecting the coolant, operating pressure, and coolant temperature. As shown in Fig .8 b), the system with liquid coolant has a less complicated structure [57], [61]. Several research studies [57], [61] were conducted to find proper liquid coolant. Mudawar et al. [57], [61] implemented several experiments among the various coolants, including perfluorocarbons (PFCs) (Fluorinerts and Performance Fluids) and HFCs (Novec fluids), to investigate the mentioned coolant requirements. According to the study results, all liquid coolants have good safety ratings. However, Fluorinerts and Performance Fluids have only average environmental ratings due to relatively high GWP [57], [61]. Overall, only HFE-7100 has good ratings in all performance categories [57], [61]. Moreover, the freezing point for HFE-7100 is 135 (°C) [57], [61], which is well below any expected automobile application range of temperatures down to 40 (°C) [57], [61]. Therefore, HFE-7100 has been recommended as a liquid cooling coolant suitable for hybrid vehicle electronics.

However, this liquid coolant with a higher boiling point requires the sub-loop to move the vapor toward the condenser for condensing to liquid. To overcome this problem and use the available coolant in the vehicle for cooling EV motors, the latest studies [23], [38] implemented a fully synthetic lubrication oil as the coolant. The study results show a high potential of the lubricant oil to be used as a coolant for the future generation of electrical motors for EV traction applications [25]. Furthermore, as shown in Fig. 8 c), the spray cooling system consists of only one close loop system with no more sub-loops and extra devices to transform the gas into the liquid. As a result, the system complexity and cost are reduced.

This closed-loop system includes coolant (oil), temperature control unit and oil tank, pump, flow control valve, spray chamber, and scavenge pump. In this cooling system, the pump boosts the oil's pressure to transfer the coolant with the appropriate pressure from the reservoir to the nozzle. Then the nozzle transforms the coolant into tiny droplets and spreads them to the hot surfaces of the end winding and rotor. In the end, the excess liquid oil is gathered with the help of a scavenge pump or just earth gravity and sent to the temperature control unit to remove the heat and prepare for recirculation.

b. Spray Nozzles Selection

The main drawback of the oil spray cooling system is the uneven temperature distribution. This drawback can cause unexpected hot spots that sometimes exceed the material's temperature limit, which leads to failures. The temperature rise distributions of a motor end region cooled by a spray system are presented in Fig. 10 to clarify the issue. Accordingly, Fig. 10 clearly shows the uneven temperature distributions at the end winding of the machine. Besides, the hairpin winding temperature rise in some slots is more than the average temperature rise and rises even more than 15 K. Therefore, the system consists of unexpected hot spots in several slots (such as 11,12, 13, 14).

In contrast, the mean temperature of the system is in acceptable conditions. As a result, the number of nozzles with the correct spray pattern must be selected during the design phase to mitigate this issue and improve the system's temperature uniformity. Hence, the various nozzles and their spray patterns are considered in detail.

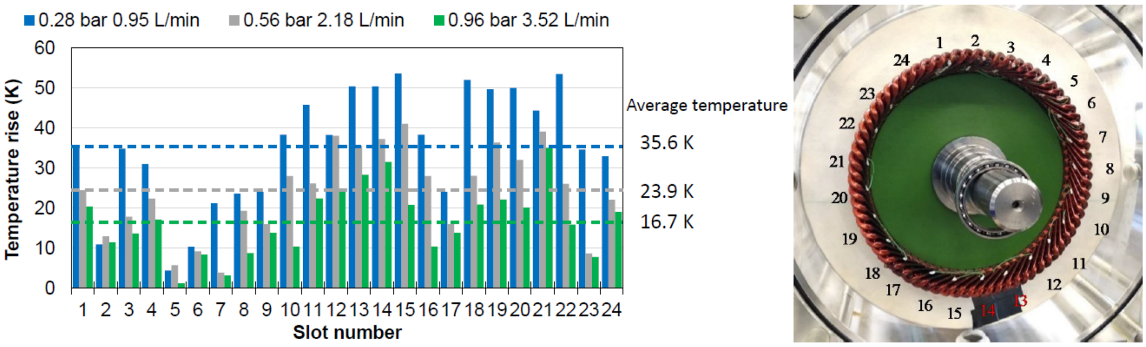

Fig. 10. Temperature rise distributions and the system's mean temperature rise cooled by the spray system under varying flow rates [25], [63].

Selecting the nozzle with the appropriate spray pattern provides excellent spreading of the coolant, which leads to more efficient cooling with better temperature uniformity. Further, the cooling system requires nozzles with high pressure. However, as shown in Fig. 11, multiple nozzles involve various applications, such as chemical processing, electronics, engineered wood, mining, fire, and safety [64], which are mainly designed to work with water. Therefore, there is insufficient information on the proper nozzles, which can work with high viscosity coolant (such as oil) and maintain their spray capabilities. Therefore, the appropriate nozzle for oil spray cooling must have the following conditions [65]:

- Proper spray pattern;
- Working with high pressure;
- Working with high viscosity coolant material.

Fig. 11. Various nozzles [64].

The procedure of selecting the nozzle contains the specification of the following items [66]:

- Spray patterns and the model of droplets spread from the orifice;
- Desired spray angle or spray coverage;
- Droplet size;
- Coolant properties;
- Material properties of the nozzles.

Hereafter, all the above parameters are considered in detail.

1. **Nozzle Spray Patterns**

The nozzle spray patterns describe the location and the spray density of the fluid emitted from nozzles. Therefore, in the first step, it is essential to know the nozzle's basic functions and working principle and then consider various nozzle types to be familiar with the different droplets' distributions.

The nozzle is a mechanical tool to transform the liquid into droplets. As Fig. 12 shows, the nozzles consist of three main functions [66]:

- Meter flow (the hydraulics of the flow within the atomizer, which governs the turbulence properties of the emerging liquid stream);
- Distribute liquid (Sheet & Ligament);
- Break up liquid stream (Drop).

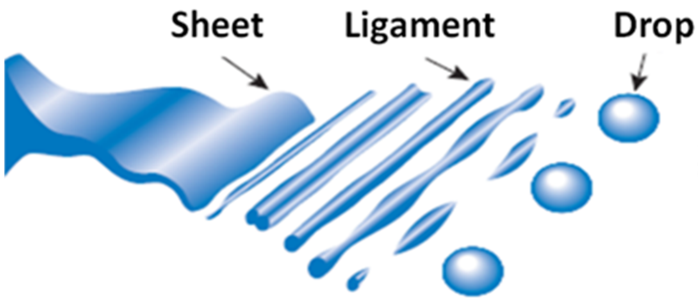

Fig. 12. The essential functions of spraying nozzles [67], [68].

In the nozzle, the process of altering the liquid into drops is called atomization, and it occurs by liquid pressure or the mixture of air and fluid pressures. As a result, the spraying nozzles are categorized into two main groups [67], [68]:

1- Hydraulic nozzles;
2- Two-fluid nozzles (air-assisted).

However, this simple sort cannot provide a complete overview of the nozzles' droplets emitting patterns. Hence, in a more comprehensive classification (as seen in Fig. 13), the spraying nozzles are categorized based on their spray pattern into four main categories as follows [54], [66]:

1- Full-cone sprays;
2- Hollow-cone sprays;
3- Flat fan sprays;
4- Misting sprays.

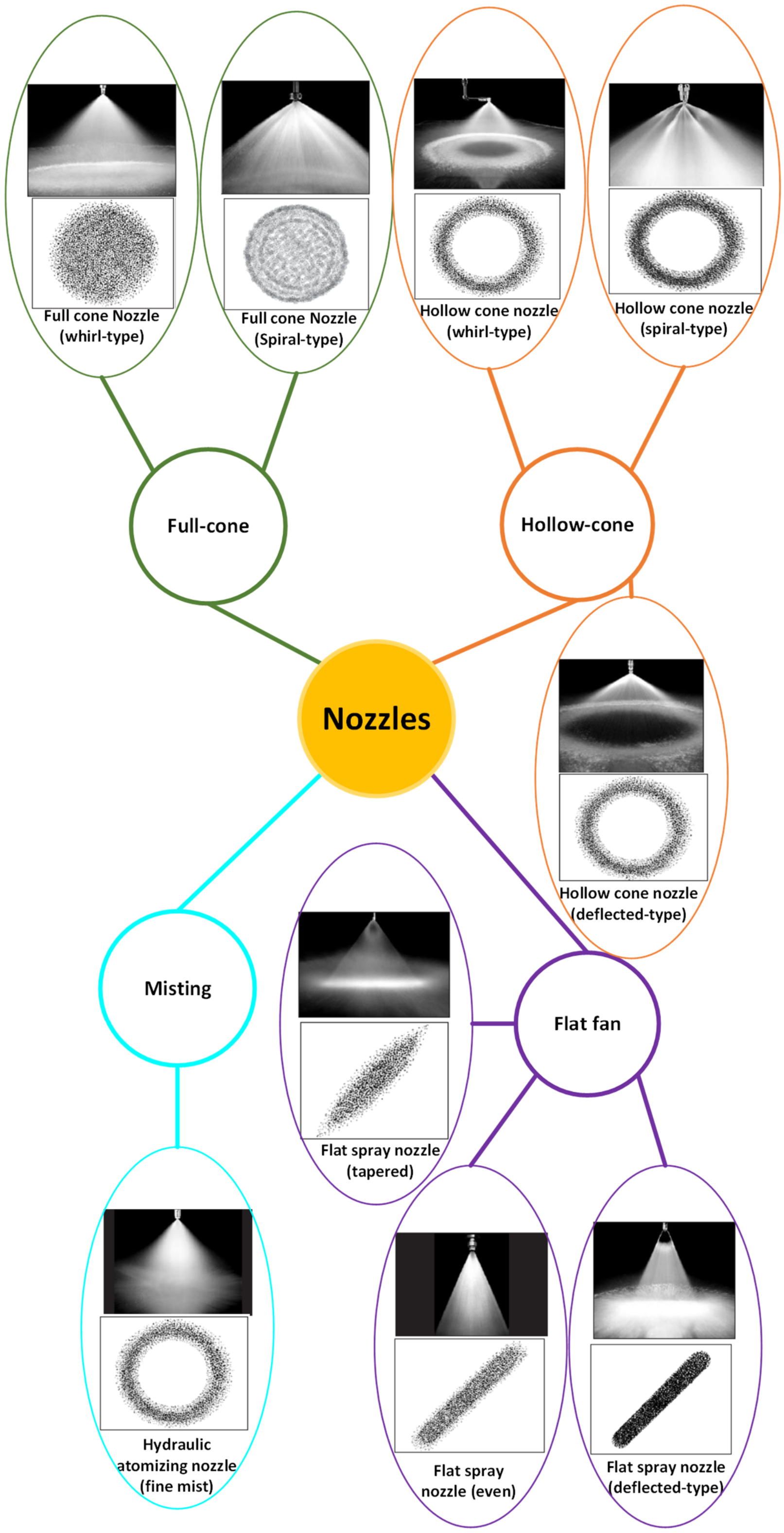

Fig. 13. Various nozzles based on spray patterns [68].

The full-cone nozzles are the most conventional in industries for spray cooling purposes. These nozzles produce various spray patterns from circular to square to oval and are generated by forcing the liquid through stationary blades that add turbulence. Therefore, these nozzles provide even fluid coverage over the target area. Besides, this pattern can be maintained for the particular distance of the target plate from the nozzle's orifice. Full-cone nozzles can have a spray angle of between 15 and 170 degrees, flow rate between 0.13 to 36100 (l/min), and pressure between 0.3 to 30 bar with medium-to-large-sized drops depending on the nozzle design [66], [70]. As illustrated in Fig. 14, the full-cone nozzle is divided into two main groups: whirl and spiral [66], [69]. As seen in Fig. 14 a), in the whirl nozzle, the fluid (coolant) is passed from the whirl chamber to set coolant in vortex motion to break up the liquid into the droplets. In the whirl full cone nozzle, droplets coming out of the orifice are evenly distributed on the target surface and shaped in the full cone pattern.

However, as shown in Fig. 14 b), the spray pattern in a spiral nozzle is generated after leaving the orifice by passing the fluid into the protruding helix [70]. Hence, the atomization process occurs after leaving the orifices. Therefore, these nozzles provide a large free passage that any contaminant passes the nozzle without causing blockage; as a result, spiral nozzles have high clog resistance and can be applied to spray a broader range of fluids [70]. Moreover, as illustrated in Fig. 14 b), the spray patterns of spiral nozzles are formed from several overlapping hollow cones with a concentric center with less uniform liquid distribution than whirl full cone nozzles to produce the full cone pattern. The concentration of heavier droplets in cones has a positive impact on delivering tiny droplets to areas that are impossible to reach by whirl nozzles, and enhances the overall cooling power of the spray [70] .

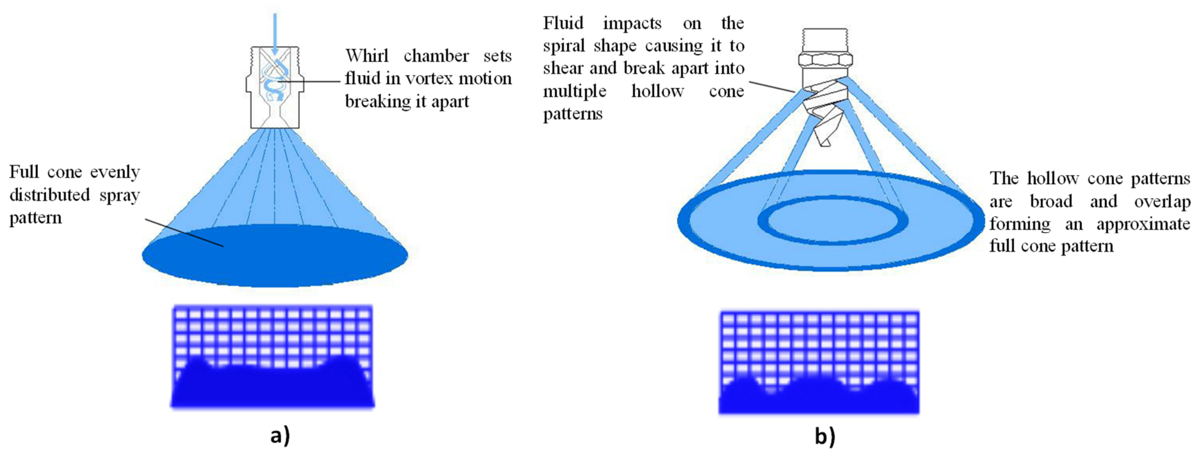

Fig. 14. Various full-cone nozzles with their distribution pattern: a) whirl b) spiral [70].

In a hollow cone nozzle, the fluid is forced tangentially from the chamber in whirl or grove vanned forms, and the exited fluid from the orifice forms the conic shape at the cone's circumference [54]. Furthermore, the spray creates a ring shape with a hollow center when it touches the surface. These nozzles can have a spray angle between 15 and 170 degrees, flow rate between 0.125 to 10700 (l/min), and pressure of 0.2 to 30 bar with a small droplet size depending on the nozzle design [70]. According to Fig. 13, the hollow cone nozzles are classified into whirl chamber, spiral, and deflected types.

As seen in Fig. 13, the flat fan nozzles produce thin and flat fluid. As it creates the fluid in concentrated form, this nozzle's effect is more significant than the previous ones and can cool the small chip area. In addition, the fluid passes minimal orifice in the misting nozzles; this nozzle produces tiny droplets even at low pressure.

Both hydraulic and two-fluid nozzles (air-assisted) can produce the above spray patterns. Besides, the two-fluid nozzle generates thinner droplets than hydraulic nozzles through a mixture of liquid and air. However, the hydraulic (pressures) nozzles are preferable for spray cooling electronic devices due to their reliance on liquid momentum to generate droplets. Moreover, two-fluid nozzles use the non-condensable gas and the liquid coolant for the atomization process, and segregating the non-condensable gas from the liquid coolant significantly enhances the cooling system's complexity [69]. Therefore, hydraulic pressure nozzles in the form of a full cone, hollow cone, and flat spray are more prevalent in many industries and spray cooling [69].

2. Spray Coverage

Another crucial factor in selecting the correct nozzles is the amount of necessary coverage. As seen in Fig. 15, the spray angle (A), actual spray coverage (B), effective spray angle (C), the distance of nozzle orifice from target area (D), and the theoretical spray coverage (E) are five main parameters that are utilized to describe the spray coverage of the nozzle [66], [71].

The spray angle (A) is determined close to the nozzle orifice. It shows the spray coverage for the surface near the orifice. However, the effective spray angle is calculated from the actual coverage (B) when the nozzle orifice is located at a specific distance (D). Finally, the theoretical spray coverage (E) shows the coverage at a distance (D) when the spray moved in a straight line.

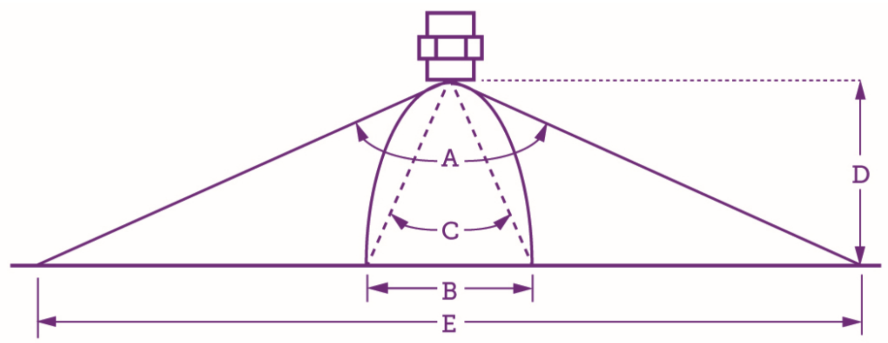

Fig. 15. Spray coverage parameters [66].

The manufacturers provide a table, such as Table II, to show the theoretical spray coverage to find the correct distance to the target surface for proper spray coverage [66]. According to the table, the spray coverage directly relates to the nozzle distance with the target surface. Accordingly, it is essential to determine the distance between the nozzle and the target surface.

Table II. Theoretical Spray coverage (E) [66].

	Distance From Nozzle Orifice (D) (Inches)											
Spray Angle (A)	2	4	6	8	10	12	15	18	24	30	36	
10°	0.4	0.7	1.1	1.4	1.8	2.1	2.6	3.1	4.2	5.2	6.3	**Spray Coverage (E) (Inches)**
20°	0.7	1.4	2.1	2.8	3.5	4.2	5.3	6.4	8.5	10.6	12.7	
30°	1.1	2.1	3.2	4.3	5.4	6.4	8.1	9.7	12.8	16.1	19.3	
40°	1.5	2.9	4.4	5.8	7.3	8.7	10.9	13.1	17.5	21.8	26.2	
50°	1.9	3.7	5.6	7.5	9.3	11.2	14.0	16.8	22.4	28.0	33.6	

3. The fluid flow rate and the impact of fluid properties on flow rate

Each nozzle generates a certain flow rate at a specific pressure differential. Hence, the flow rate is determined by subtracting the gauge pressure inside the vessel from the gauge pressure at the nozzle inlet and is expressed as [66], [70]:

$$Q = K(P)^n, \quad (1)$$

where Q is the flow rate (l/min), K is the coefficient factor, P is the pressure differential, and n is a constant.

Therefore, the following correlation is used to calculate the flow rate of fluids with various pressures [66]:

$$\frac{Q_2}{Q_1} = \left(\frac{P_2}{P_1}\right)^n . \quad (2)$$

The coefficient factor (K) is a unique number for each nozzle provided by the manufacturer in the datasheet. n is a constant that mainly depends on spraying patterns; for instance, this value for most spiral full cone nozzles is 0.5 and is between 0.44 to 0.46 for whirl types [66], [70].

Most of the nozzles in the market are being designed to work with water; the flow rate chart provided in the manufacturer datasheet presents the value of flowrate on the specific pressure differential for the water as fluid. Therefore, it is necessary to recalculate the flow rate for heavier or lighter fluids than water. For this purpose, the effect of the fluid parameters such as viscosity and specific gravity (SG) on the spraying must be considered for the high dense coolant. Therefore, the following correlation is used to calculate the flow rate of fluids with various SG [66]:

$$\frac{Q_2}{Q_1} = \sqrt{\frac{SG_1}{SG_2}} . \quad (3)$$

Table III shows the water and engine oil's viscosity and specific gravity (SG). Therefore, by replacing the water-specific gravity (SG=1) for SG_1 in (3) and defining Q_1 as the water flow rate (Q_W) in (4), it can be determined the fluid flow rate (Q_F) by knowing the water flow rate [70]:

$$Q_F = Q_W\sqrt{\frac{1}{SG_2}} . \quad (4)$$

Table III. Viscosity and specific gravity at room temperature [66]

Fluid	Viscosity (cP)	Specific Gravity
Water	1	1
10W-30 oil	110	0.88

According to (4), the viscosity and the specific gravity impact the spray performance differently. The viscosity mainly increases the energy required for the atomization process. For example, the high viscosity liquid can interrupt the spraying capability. In a critical situation, air atomizing nozzles are the only nozzles used to spray the high viscosity liquid. Generally, high viscosity [67]:

- Decreases flow rate;
- Creates heavy edges;
- Requires a higher minimum pressure to maintain adequate spray angle/coverage;
- Increases capacity;
- Increases drop size.

4. **Droplet Size:**

The different nozzles produce various droplets. Depending on the nozzle type, the droplet size varies significantly from one type to another. Generally, the air atomizing nozzles or spiral air series generate the smallest droplets, followed by hollow-cone, flat fan spray, and full-cone nozzles.

The size of the droplets can describe the overall surfaces that can be covered by sprayed fluid. Smaller droplets increase the surface area of the spray [70]. In addition, the droplet size plays a vital role in developing empirical correlations to measure spray cooling performance. The various studies on spray cooling developed an empirical correlation and analytical model using dimensionless numbers under multiple conditions during the past few decades. Therefore, most of these correlations require the knowledge of mean droplet size as the characteristic length.

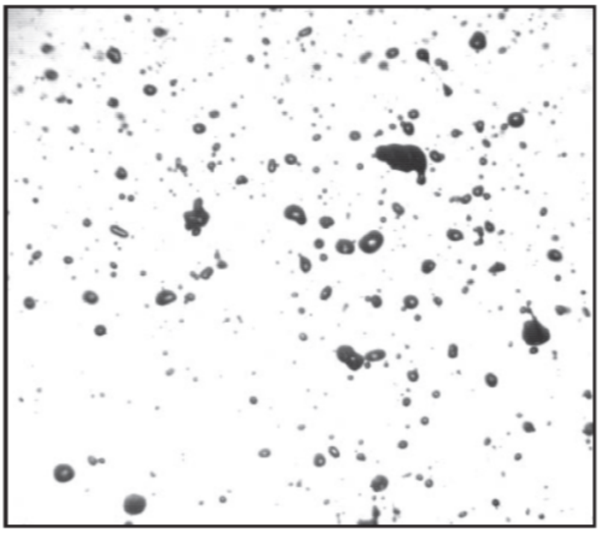

Fig. 16. Actual droplet image for spray analysis [66].

4.1. Droplet size measurement

The droplet size measurement is critical and challenging since there are numerous drops in spray, including vast drop sizes—furthermore, the drop size changes by moving toward a two-phase regime due to evaporation and coalescence. The droplet size can be measured by different methods like mechanical, electrical, and optical [67], [68], [72], [73]. As seen in Fig. 16, the spray nozzle generates a wide range of droplet sizes; hence, a single number is defined as the droplet size. Moreover, this number is used in comparisons of droplets of various sprays. Therefore, the diverse average numbers are defined for the droplet sizes.

Further, many applications are more comfortable using the mean number [67]. Different mean numbers are generalized in [74]. Generally, the mean diameters are described by the below correlation [67], [75]:

$$(D_{ab})^{a-b} = \frac{\int_{D_0}^{D_m} D^a\left(\frac{dN}{dD}\right)dD}{\int_{D_0}^{D_m}\left(\frac{dN}{dD}\right)dD}, \quad (5)$$

where a and b are the positive integer numbers, D_m is the maximum drop diameter, D_0 is the minimum drop diameter, D is the drop diameter, and N is the number of drops. Furthermore, equation (5) can be defined as [75]:

$$D_{ab} = \left[\frac{\sum N_i D_i^a}{\sum N_i D_i^b}\right]^{1/(a-b)}, \quad (6)$$

where i presents the size range considered, N_i equals the number of drops on size range i, and D_i is the middle diameter of size range i. According to (6), various mean diameters can be defined. Table IV provides the different mean diameters and their applications. For more information, the common ones are as follows:

- Arithmetic mean diameter (D_{10});
- Volume mean diameter (D_{30});
- Sauter mean diameter (D_{32});
- De Brouckere mean diameter (D_{43}).

Table IV. Mean diameter and their applications [67], [74]

a	*b*	*a+b*	Title of mean diameter	Symbol	correlation	Applications
1	0	1	Length (arithmetic mean diameter)	D_{10}	$\frac{\sum N_i D_i}{\sum N_i}$	Comparisons, evaporation
2	0	2	Surface area	D_{20}	$\left[\frac{\sum N_i D_i^2}{\sum N_i}\right]^{1/2}$	Surface area controlling, e.g., absorption
3	0	3	Volume	D_{30}	$\left[\frac{\sum N_i D_i^3}{\sum N_i}\right]^{1/3}$	Volume controlling, e.g., hydrology
2	1	3	Surface area-length	D_{21}	$\frac{\sum N_i D_i^2}{\sum N_i D_i}$	Absorption
3	1	4	Volume-length	D_{31}	$\left[\frac{\sum N_i D_i^3}{\sum N_i D_i}\right]^{1/2}$	Evaporation, molecular diffusion
3	2	5	Sauter mean diameter (SMD)	D_{32}	$\frac{\sum N_i D_i^3}{\sum N_i D_i^2}$	Mass transfer, reaction
4	3	7	De Brouckere or Herdan	D_{43}	$\frac{\sum N_i D_i^4}{\sum N_i D_i^3}$	Combustion equilibrium

4.2. Impact of spray and fluid parameters on droplet size

The droplet size is directly proportional to the nozzle's internal geometry, orifice size, physical properties of a liquid, spray angle, and spray pressure. According to the effect of droplet size on the spray performance, it is essential to consider the impact of these parameters on the droplet sizes. Hereafter the impact of these parameters on droplet size is investigated [66], [70].

4.2.1. Fluid Parameters

This part investigates the effect of fluid parameters such as pressure, specific gravity, viscosity, and surface tension on the droplet size. All these parameters impact the flow rate and the spray ability of the nozzles [66], [70].

Pressure directly impacts the droplet size, which means that the droplet size becomes smaller by increasing the fluid pressure. Besides, it is suitable to predict the droplet mean diameter by changing the pressure; hence the following equation expresses the effect of pressure on the mean diameter droplet size [66], [70]:

$$\frac{D_2}{D_1} = \left(\frac{P_2}{P_1}\right)^{-0.3} . (7)$$

where D_1 and D_2 are the mean diameters of droplets at pressure one (P_1) and pressure two (P_2), respectively.

The specific gravity affects the liquid flow rate, and as a result, it affects the droplet size, which means that for the same pressure, the higher SG leads to a lower flow rate and smaller droplet size. Therefore, the mean droplet diameter can be determined as follows [70]:

$$D_F = D_W SG_F^{0.3},(8)$$

Moreover, the fluid viscosity (V_F) affects the nozzle's performance, and the liquid with high viscosity can inhibit the atomization process. Hence, a fluid with high viscosity increases the droplet size, and the mean diameter of fluid can be evaluated as follows [70] :

$$D_F = D_W V_F^{0.2},(9)$$

Similar to fluid viscosity, the fluid with higher surface tension (S_T) forms the larger droplets, and the droplet mean diameter can be estimated as follows [70]:

$$D_F = D_W \left(\frac{S_T}{73}\right)^{0.5}, (10)$$

4.2.2. Nozzle Parameters

The nozzle type, spray pattern, and spray angle affect the droplet size. Typically, the nozzles with lower atomizations, such as flat fans with patterns of liquid sheets, generate the coarse droplets. Moreover, the nozzles with a broader spray angle generate the smaller droplets since they provide more space for the distribution of droplets. Besides, the type of nozzles also affects droplets' size; for example, the spiral full cone nozzles produce smaller droplets than whirl ones.

5. The material properties of the nozzles

The environmental conditions and coolant features such as ambient and working fluid temperature, corrosion, oxidizing, chemical attack, and abrasion play an essential role in selecting the nozzle-constructed materials and maximum working temperature limit of a nozzle. Furthermore, these parameters impact the nozzle cost and the product's final price. The nozzle-constructed materials based on the cost from highest to lowest price are sorted as follows: refractory metals and precious metals, ceramics, nickel-based alloys, cobalt-based alloys, stainless steels, plastics, cast iron, and brass [66].

The critical and challenging factors in the spray cooling approach are the system's complexity and temperature uniformity. Recently, lubricant oils have been utilized as coolants to reduce the system complexity. However, as coolants, these fluids have higher viscosity and lower specific gravity than water. Since a high viscous liquid reduces the atomization process and performance of the nozzles, for this purpose and for mitigating the temperature non-uniformity, the essential coolant parameters and their effects on the nozzle's performance, various nozzles, and their spray patterns need to be considered.

Since most nozzles are designed to work with water, most manufacturers provide the amount of flow rate charts and spray angle of the nozzles for the water as fluid. Therefore, it is essential to recalculate parameters, such as flow rate at a specific pressure, nozzle spray covers, and spray angles for lubricant oil as fluid. Then, select the proper nozzle according to the amount of the recalculated parameters, spray coverage, and the nozzle's distance from the targe surface. Moreover, Table V summarizes the nozzles with their patterns, spray angles, flow rate, pressure, and the size of droplets.

Table V. Overview of various nozzles and their parameters [66], [70].

Nozzle Type	Spray patterns	Spray angle range (degree)	Flow rate range (l/min)	Liquid Pressure Range (Bar)	Drop Size
Hydraulic Full-cone	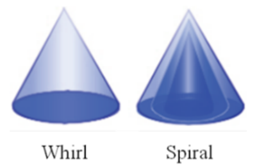	15°-170°	0.13-36100	0.2-30	Medium to Large
Hydraulic Hollow-cone	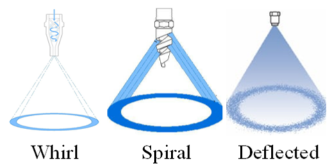	15°-170°	0.125-10700	0.2-30	Small
Hydraulic Flat fan	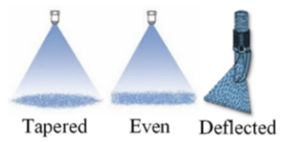	0°-145°	0.011-757	0.2-40	Small to Medium
Hydraulic Misting	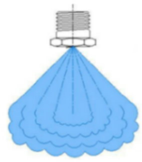	20°-120°	0.032-618	0.7-200	Small
Two-fluid nozzles	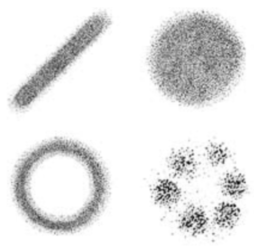	10°-90°	--	0.2-7	Very Small

III. Oil Spray Cooling Approach in Electrical Motors for Traction Drives

Using spray cooling on electrical machines is a novel approach. But, the spray cooling method itself is not novel; there are numerous research studies about the spray cooling approach [69], [76]-[78]. Moreover, this cooling method has a complex heat transfer mechanism, for which most of the findings are based on the experimental way. However, these findings mainly concentrate on thermal engineering devices instead of windings; such as evaporative spray cooling of silicon surfaces textured with square micro-study, water spray cooling performances of plain and micro-porous coated flat and cylindrical surfaces, PF-5060 spray cooling performances for different structured surface geometries: cubic pin fins, pyramids, and straight fins [69]. Consequently, they are less applicable to electrical machines. most of them concentrated on tasks

As shown in Fig. 17, the attempt and research data to implement an oil cooling system on electrical machines are categorized into two main groups: evaporation spray cooling and lubricant oil spray cooling. Moreover, lubricant oil spray cooling is divided into two subsections according to the motor winding configuration: lubricant oil spray system on motors with strand windings, and motors with hairpin windings. Finally, the strand winding configurations based on nozzles positions are divided into two other subsections. All attempts and research to implement the spray cooling system on electrical machines together with its advantages and drawbacks are described here.

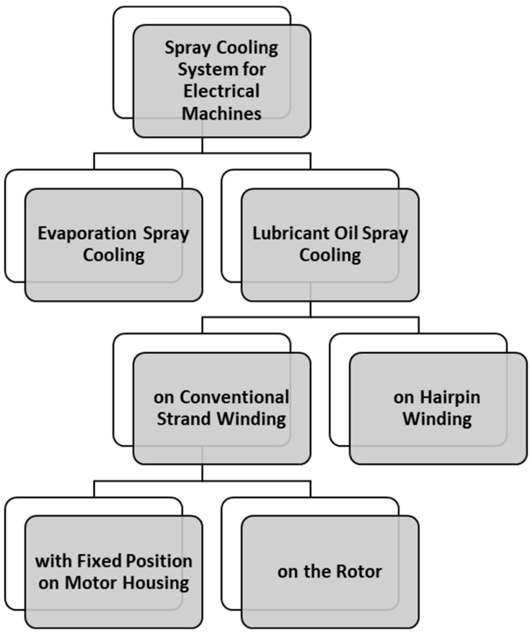

Fig. 17. The attempt and research on implementing of oil cooling system for electrical machines.

a. Evaporation Spray cooling system on electrical machines

Early research on utilizing a spray cooling approach for electrical machines dates back to 2009, when Li Zhenguo et al. [49] implemented an evaporation spray cooling on a sizeable synchronous generator. Conventionally, this type of generator is cooled using a wet stator method by immerging the stator part into the coolant. However, the drawback of this cooling is the requirement of a large cooling medium.

Therefore, to reduce the quantity of the cooling medium, the spray cooling systems were implemented in the stator active part and stator end regions.

For this purpose, nozzles with spray angles of 15~45°; a flow rate of 2.5L/min at 0.05Mpa were installed in the machine. Furthermore, F-113 with a low boiling point was used as an evaporation coolant; therefore, the system mainly concentrates on a two-phase cooling. As seen in Fig. 18, the thermal management system consists of a condenser, pumps, nozzles, filters, a coolant distributor, flow transducers, spray rings, and electromagnetic valves. Besides, they used an insulation sleeve to separate the wet stator chamber from the dry rotor chamber. Consequently, the cooling system consists of several subloops that increase the complexity and cost of the cooling system. Nevertheless, according to the findings, this thermal management system reduces coolant usage to about 90%. Moreover, compared to the semi-flood method, the spray cooling approach provides better cooling capabilities, smaller coolant inventory, and better temperature uniformity.

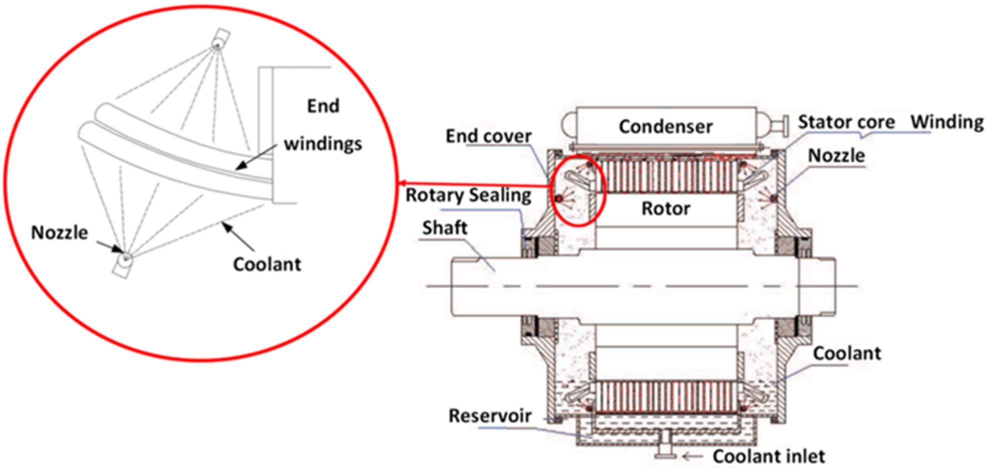

a)

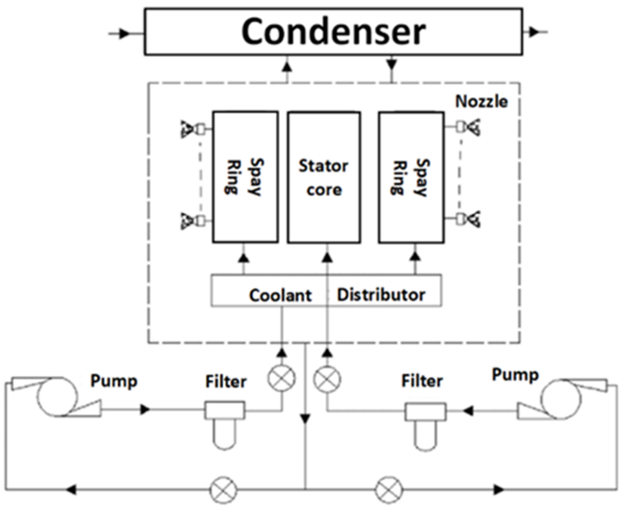

b)

Fig. 18. Implementation of spray cooling in a large electrical machine: a) Test rig b) Fluid system setup [48], [49].

Li Zhenguo et al. in [48] consider the challenges of evaporation cooling systems, two-phase heat transfer, and the effect of critical spray parameters on the heat transfer capabilities and thermal management system's efficiency through experiment. For this purpose, they designed the test rig (Fig. 19), including the *motorette* (a small representative section of the stator) located inside the chamber. As seen in Fig. 19, the *motorette* consists of four radial cooling ducts cooled by full cone nozzles installed above the end windings and the stator radial cooling ducts.

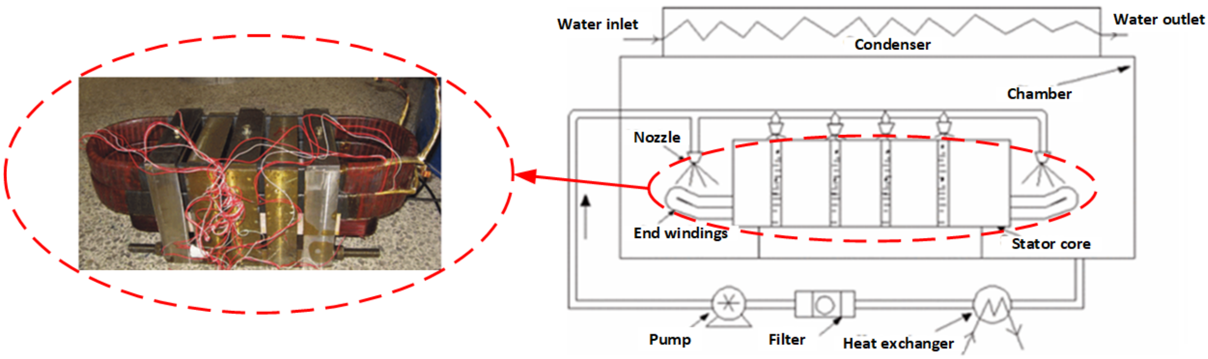

Fig. 19. The schematic of the test rig [48].

Table VI shows the effects of pressure and coolant temperature on the spray cooling system performance. Section II states that pressure directly relates to flow rate and is inversely proportional to mean droplet diameter. Their findings show that increasing the pressure directly impacts the flow rate, heat transfer coefficient, and cooling efficiency. Therefore, increasing the pressure leads to better cooling and lower temperature. Accordingly, by increasing the pressure from 0.7 bar to 10 bar, the flow rates increased from 1 l/min to approximately 4 l/min, droplet size decreased from 2.1 mm to 0.6 mm, and the windings' temperature dropped from 90 °C to approximately 60 °C. Besides, this temperature reduction continues until a particular pressure (5 bar), and after that pressure, by reducing the thickness of the liquid film on the winding surface, the temperature is not reduced sharply as before. However, increasing the pressure has an opposed effect on mean droplet size and leads to smaller droplet size.

In the final step, the impact of the inlet temperature of evaporation fluid on the heat transfer and temperature of the system was investigated. As a result, if the coolant temperature is far lower than its saturation point, spray cooling system efficiency and heat transfer coefficient drop and lead to higher windings temperatures.

Table VI. The effect of critical spray parameters on the heat transfer capabilities and thermal management system efficiency.

Parameter	Fluid Flow	Mean Droplet Diameter	Winding Temperature	Heat Transfer Coefficient	Cooling System Efficiency
Increasing Pressure	⬆	⬇	⬇	⬆	⬆
Decreasing Coolant Temperature	—	—	⬇	⬇	⬇

The final part of the research on the two-phase evaporation system is presented by Li Zhenguo et al. in [79], where they investigate various sprays and the effect of their parameters on the high power density motor cooling. For this purpose, they constructed an experimental platform (Fig. 20) consisting of a spray cavity with the nozzle, heater, sub-cooling, pump, preheater, condenser, and control system.

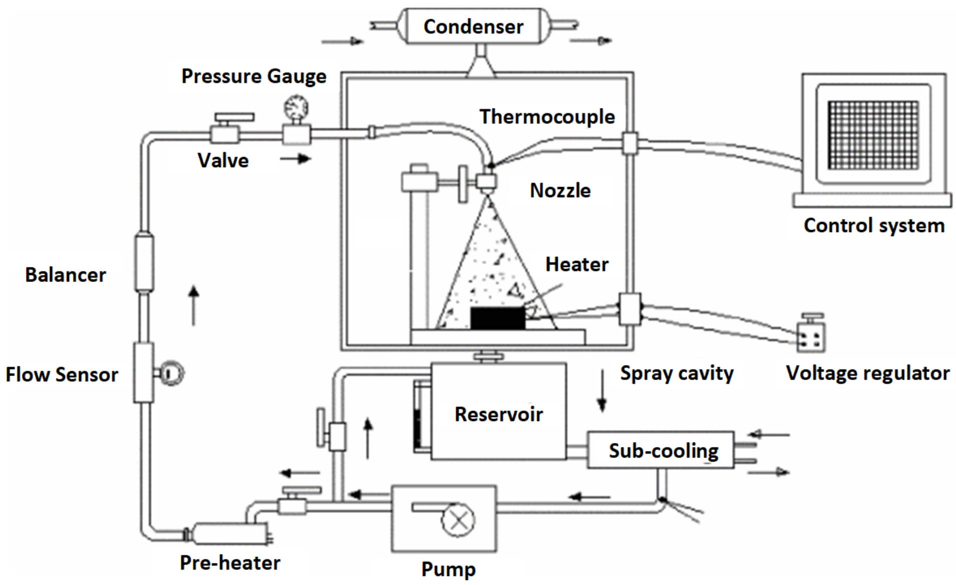

Fig. 20. The test bench schematic [79].

They utilized four different nozzles with different orifice sizes and spray angles installed at a 70 mm distance from the heating object. As a primary goal, they considered the behavior of the heat transfer coefficient via pressure variation for the nozzles to select the nozzle with the best evaporation spray cooling capacity. As seen in Fig. 21, the rate of heat transfer coefficient increases by enhancing the pressure in all nozzles, and it has a positive effect on the heat transfer and cooling efficiency. Since nozzle#3 has the best performance in heat removal, for further investigation, they selected this nozzle to consider the impact of various parameters on the evaporation spray cooling capacity, such as nozzle distance from the heating object, spray inclined angle, and inlet coolant temperature.

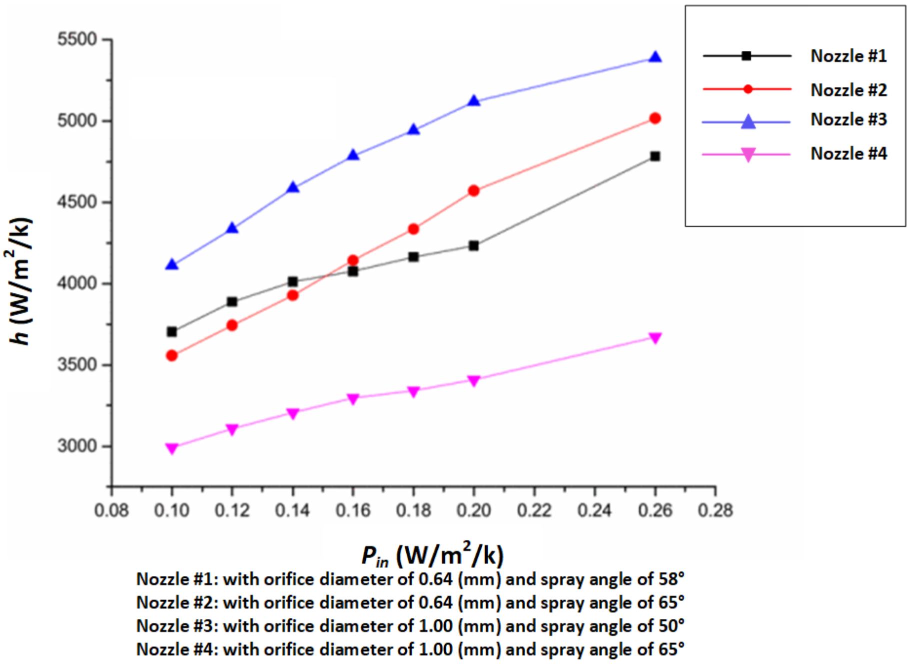

Fig. 21. Variation heat transfer coefficient via input nozzle's pressure [79].

First, they considered the effect of the nozzle's distance on the heat transfer coefficient. Based on their findings, the heat transfer coefficient until a certain distance from the heating object (40 mm) was increased and after exceeding this distance started to decline. In the next step, they checked the effect of inclined spray angle on the heat transfer capability. According to their findings, the inclined spray angle has a significant impact on the heat transfer coefficient; as an example, for the nozzle under experiment, by increasing the inclined spray angle from 0 to 20 degrees, the heat transfer coefficient increased about 9%, and it reached to its maximum value (about 5700 W/m^{2}K). However, by increasing the inclined spray angle from 20 degrees, the heat transfer coefficient sharply decreased, and at 50 degrees, the heat transfer coefficient dropped to 4200 W/m^{2}K. Furthermore, they compared the evaporation spray cooling capacity with the immersing liquid technique and realized that spray cooling provides a higher heat removal capability (around 10%) by comparing the spray and immersion cooling methods at the same heat fluxes.

b. Lubricant Oil Spray cooling system

The above studies have not provided any information about nozzles with various spray patterns. They only focus on the full cone nozzle for sizable machines with evaporation coolant. In contrast, EV motors are compact and installed in tiny places. Therefore, there is no adequate space for installing extra devices such as pre-heat, extra pumps, condenser, and reservoir for evaporation coolant. Furthermore, the cooling system's primary objective is to use the available fluid as a coolant; for instance, in EV motors, the coolant can be air, water, and oil. As a result, the lubricant oil with a more straightforward thermal management system, including one loop, becomes suitable for EV motors.

1. EV motors with strand windings and fixed nozzles positions

Davin et al. [37] present one of the early studies considering implementing oil spray cooling in EV traction (powertrain) motors. In [7], [37], they implemented this cooling approach on both sides of the motor with concentrated strand windings and proposed the inverse method to determine the value of interior heat transfer coefficients.

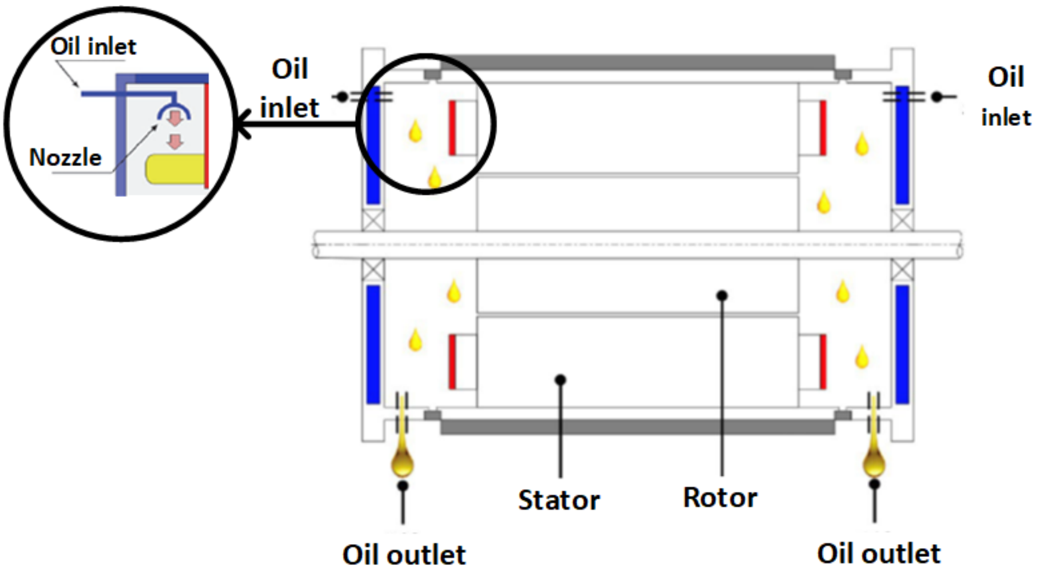

Fig. 22. Schematics of the test machine by Davin et al. [37].

According to Fig. 22, they utilize the lubricant oil to spray on both sides of the motor by installing two different injection systems. The first system used the atomization spray (Mist) system consisting of a whirl full-cone (M8) and flat jet (HVV04) spray nozzles with a fixed location on the top of the housing to cool the stator end windings directly. The second system was based on a solid stream injection technique (a simple jet of focused fluid with no actual droplets) consisting of Dripping and multijets to distribute lubricant oil around the outer periphery of end windings. Afterwards, lubricant oil is sorted from the machine at the bottom through gravity and back to the temperature control unit to recirculate. The oil spray system is implemented on a real stator with a nonmagnetic rotor to control the heat transfer and restrict the machine's power losses.

They considered the influence of oil flow rate and rotor rotational speed on the cooling system performances. Fig. 23 shows the experimental results on all four injection systems topologies. As seen, the misting systems have a lower flow rate domain compared to the solid stream systems. Overall, increasing the oil temperature has a positive impact on heat removal. Therefore, increasing the oil flow rate improves the cooling system performance in all four spray topologies, causing more heat power removal and lowering windings' temperature. Besides the significant densification of droplets at high pressure and flow rate, the powerline's slope is sharper in spray atomization systems than in solid stream injection systems. The other interesting point is the better performance of dripping systems with few injection points compared to multijets.

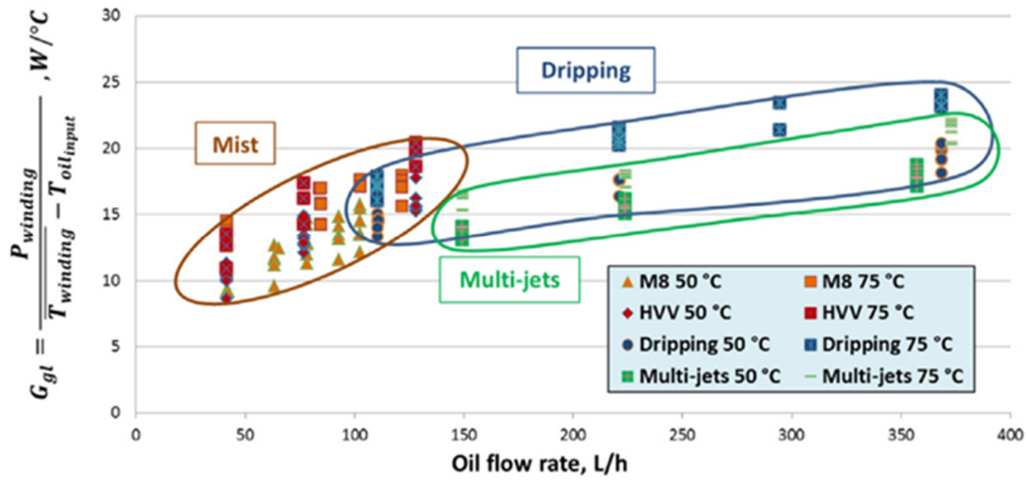

Fig. 23. Impact of various spray systems on the windings' temperature and dissipated power [37].

Moreover, the rotor speed positively affects the heat removal and causes heat transfer improvement. This effect is noticeable for mist nozzle topologies (full cone and flat jet nozzles) and moderate for multijet and dripping systems. However, as shown in Fig. 24, the non-uniformity of oil film distribution on end windings during high rotor speed becomes more significant, leading to uneven temperature distribution on the end windings. The main drawback of the uneven temperature distribution is the occurrence of unexpected hot spots in the system. In this research, in some measurement cases, there was a temperature difference of more than 30°C in various parts of the machine; they even observed a 20 °C temperature difference within the same winding.

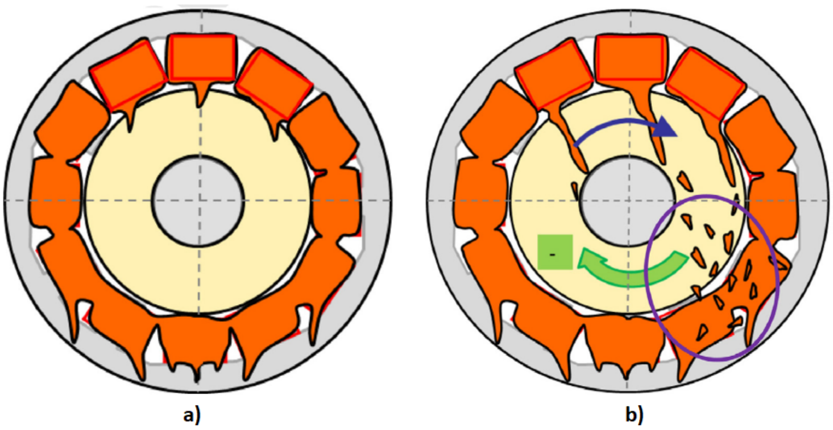

Fig. 24. Sketch of flow visualization: a) at stall condition and b) higher rotor rotational speed [37].

Bennion and Moreno in [80] present a research study of the oil spray cooling on the electrical motor for traction drives. They propose the direct end winding cooling by accomplishing impinging automatic transmission fluid (ATF) jets onto the motor's end winding. They experimentally consider the effect of the inlet coolant temperatures, flow rate (jet velocities), and the surface topology on the machine's heat transfer coefficient (HTC) and pressure drop (PD) across the nozzle. Therefore, for the impact of inlet coolant temperatures, ATF temperatures vary from 50°C to 90°C, and for the flow rate analysis, jet nozzle velocities vary from 0.5 m/s to 10 m/s. Ultimately, they utilized various wire bundles called the baseline, 18 AWG, 22 AWG, and 26 AWG samples to consider the influence of surface topology. Table VII presents their findings and observations. Besides, this cooling approach proposed high heat removal and high HTC; for instance, at the jet velocity of about 10 m/s, the HTC is between 8000 – 10,000 W/m^2K.

However, in this current study, they only use the small copper wire sample that is directly aligned with the fluid jet. In actual conditions, the end winding is on a larger scale with a bigger surface; therefore, all the surfaces cannot be directly impinged upon by the jet and face a non-uniform heat transfer condition.

Table VII. Results on the impact of surface topology, fluid temperature, and jet velocity on pressure drop (PD) and heat transfer coefficient (HTC).

	PD	HTC
Flow rate (Jet velocity)	By increasing the flow rate, the pressure drop also increases	HTC increases with increasing jet velocity
Inlet coolant temperature	It decreases with increasing inlet temperatures	The inlet temperature has a negligible impact on HTC
Surface topology	----------------------------------	-Low jet velocities (less than 0.5 m/s) have minimal effect on HTC, and the values of HTC for all the samples were identical. -At higher velocities, HTC values for 18 AWG and 22 AWG were more significant than the two others

2. EV motor with strand windings and installed nozzle on the rotor

Hitherto, several cases are considered for which the spray cooling method was accomplished by fixing nozzles on the machine housing's interior sections. However, several research studies assessed the effect of oil spray cooling arrangement by utilizing the spray system on the rotor shaft for in-wheel (hub) motors for light hybrid electric vehicles [81]-[85]. These motor types are installed directly in the machine wheels, and each motor is controlled individually by its motor drive [83], [85]. Therefore, the vehicle's kinematic performance and design flexibility are increased [83]. Moreover, in comparison to traction motors, this system does not require any mechanical links, such as transmissions or differentials

[85]. However, the negative point about this motor system is the limited space, since the in-wheel motor and its drive, together with other wheel accessories, such as a braking system, steering system, and suspension, are installed in a tiny wheel space [83]. Therefore, this motor system needs to be minimized.

Moreover, due to the complex structure of this system, selecting the correct thermal management system is crucial to provide high performance and durability. However, the conventional air-cooling approach and water cooling are not suitable thermal management systems for large-capacity drive motors. The air cooling method cannot provide sufficient cooling capacity, and the water cooling approach needs a separate flow path in the machine housing, contrasting with motor size minimization [83]. Hence, the spray cooling from the rotor shaft is a thermal management system that can overcome these issues [83]. As seen in Fig. 25, Lim et al. [82], [83] conducted one of the primary studies by optimizing the cooling channel inside the hollow shaft for implementing the oil spray cooling into a 35 kW in-wheel motor. In the first step, they use the Taguchi technique to optimize the channel and flow path of the hollow shaft. Then, they considered the thermal performance of the optimized motor by utilizing numerical analysis and experimental methods. Finally, they evaluated the thermal performance of the optimized motor under the base and maximum operating speeds, and various operating conditions of the cooling system.

According to their findings, oil spray cooling provides better cooling performance and temperature uniformity than air-cooled and oil-cooled methods. Moreover, using a spray cooling system, they set the maximum temperature of the in-while coil under the motor temperature limit (motor temperature limit set to 150 °C). As a result, the coil temperature for base speed and maximum speed performance were 138.1 °C and 137.8 °C, respectively.

Furthermore, in [83], they evaluate the heat extraction and thermal performance of the 35 kW in-wheel motor in the presence or absence of the radiator in the circulation loop of the oil spray cooling system. They observed that the rate of temperature rise of the model with the radiator in the cooling loop system is about 30 °C/min lower than for the condition where the radiator is not included under the maximum rated base speed condition, and it is possible to secure additional driving time of about 22 s. However, they did not provide any information related to HTC.

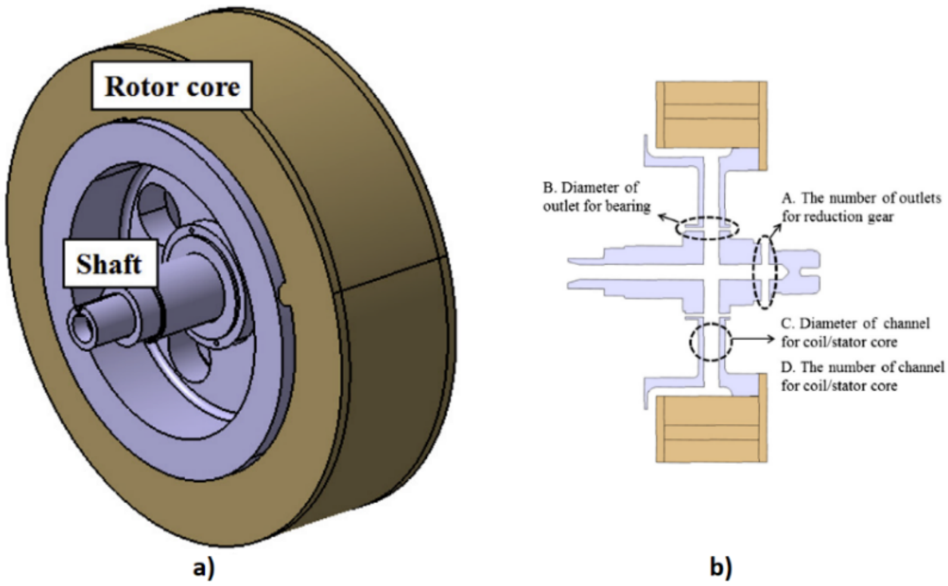

Fig. 25. a) The in-wheel motor construction, b) The optimization parameters [82].

Park and Kim in [84] presented the latest study on implementing the oil spray cooling system on the rotor shaft of an in-wheel motor. As seen in Fig. 26 a) and b), they designed the new hollow shaft with several oil channels for direct spray cooling and delivering oil for lubricant purposes. Fig. 26 c) illustrates the spray coverage with the oil spray cooling technique. Therefore, spray cooling techniques was only implemented in the non-drive end windings, and the driven parts were cooled by the oil flowing from the non-drive end part due to rotor rotation and gravity.

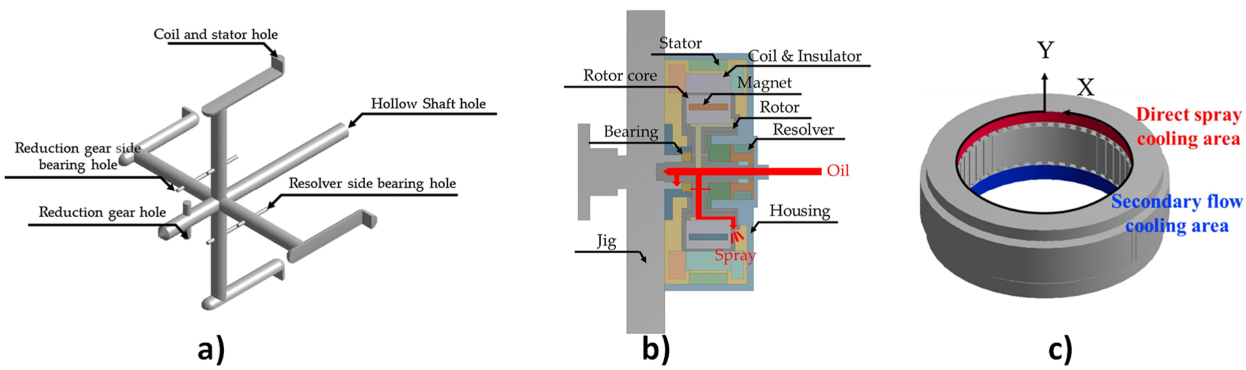

Fig. 26. Structural modeling of a) cooling channel, b) in-wheel motor with hollow shaft spray cooling, and c) spray cooling area at coil and stator [84].

Next, they evaluated the oil spray system's performance for the 35-kW interior permanent magnet (IPM) motor with the optimized hollow shaft. According to their findings, the average HTC for the direct spray cooling in the non-drive end section at base speed and maximum speed performances are about 5270 ($W/m^2/K$) and 10849 ($W/m^2/K$), respectively. Then, they compared the spray cooling system's performance with the conventional cooling system, such as an in-wheel motor with only a simple channel cooling, stagnant, and circulating at the base and maximum speeds. According to their observation, the coil absolute temperature by implementing a spraying cooling system at base speed was 25.0%, 11.6%, and 15.8% lower than simple channel cooling, stagnant, and circulating methods. Furthermore, as illustrated in Fig. 27, at the base speed, the average HTC of the oil spray cooling is 21 times greater than the simple cooling channel, and at maximum speed, this value is 22.5 times higher than the simple channel cooling. Consequently, oil spray technique has a significant impact on the thermal performance of the cooling system of an in-wheel motor.

As seen in Fig. 27, the cooling system performance mainly depends on the rotor speed. Therefore, the drawbacks of the oil spray cooling system on the rotor shaft are that it may not provide good oil atomization and offer perfect oil film in some parts, leading to a temperature hotspot in some portions. Furthermore, according to Fig. 27, at maximum speed, the variation of HTC along the perimeter of the direct spray cooling area of the coil is considerably reduced compared to base speed due to the injection force at high-speed conditions, which leads the spray droplets to cover more uniformly the surface, which increased the oil film's cooling impact.

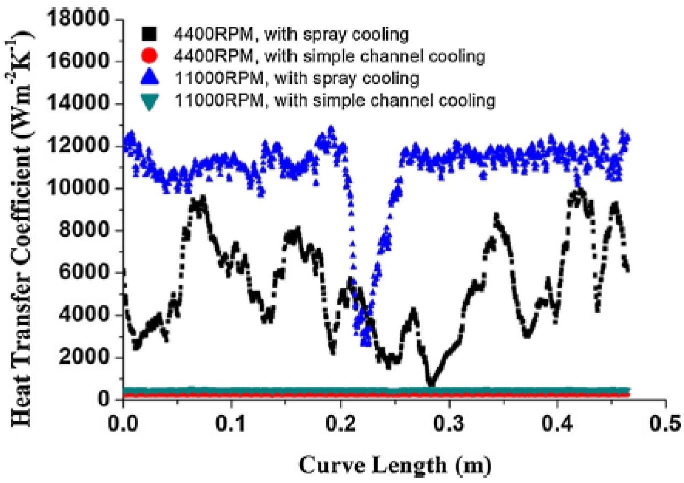

Fig. 27. Numerical results of HTC at direct spray cooling area [84].

Furthermore, the research studies presented in [82], [84], and [86] are one of the few studies in the field of oil spray cooling of electrical machine that benefits from numerical analysis, including computational fluid dynamics. Besides, by comparing the numerical with experimental results, as seen in Fig. 28, they agree with the maximum error of 5.7% for the stator and 7.9% for end winding. As an example, at 11000 RPM, the winding temperature obtained by the numerical and experimental methods are 408 K and 410.8 K, respectively.

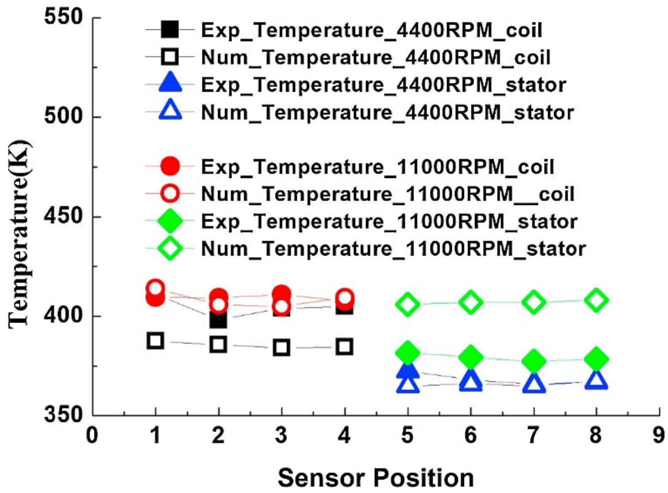

Fig. 28. Numerical and experimental results of the stator core and end windings for the in-wheel motor with an oil spray cooling approach [84].

3. EV motor with hairpin windings

The practical option for achieving the demanded metrics, such as maximizing electric motors' power and torque density and minimizing the motor's weight for traction applications, is replacing the traditional round-wound wires with rectangular hairpins [87], [88]. Therefore, in the coming years, hairpin windings technology is recognized as the standard solution for high-reliability motor drives for hybrid electric vehicles [25], [50], [53]. Moreover, the oil spray cooling approach is a cooling system that perfectly matches motors with hairpin windings. In the conventional strand windings, the impregnation materials such as resin fill the gap among the end windings, and the coolant is only in contact with the outer or inner surface of the end windings. Contrary to conventional strand windings, the end winding part of a hairpin configuration consists of the pre-determined gap that is not filled and the oil as coolant is in direct contact with all the periphery of the conductors and provides better cooling. Besides, this type of winding includes the copper bars, which provide considerable axial heat transfer. Moreover, according to the small number of conductors inside the slot with an approximately clear position and a small temperature gradient across the rectangular conductor area, it is not necessary to calculate the equivalent thermal conductivity of the slot during thermal modeling and analysis.

Several research studies consider the effect of oil spray cooling on hairpin windings. However, the latest and most comprehensive studies on the direct oil spray cooling approach on the end parts of the hairpin winding's configuration have been conducted through collaborative work between the University of Nottingham and Motor Design Limited company [25], [38], [89]-[91]. As seen in Fig. 29 a), they developed a test rig to consider different spray cooling setups' capabilities. For this purpose, they selected a stator with 72 slots with a hairpin winding configuration. Besides, they fit the stator and non-drive end winding into the encapsulated cover, and the drive end part of the machine is fitted inside the cover made of Perspex material. Fig. 29 b) shows the fluid system setup, with various apparatus to provide the spray cooling and investigate the effect of different parameters such as flow rate, outlet velocity, and the number of nozzles on the cooling capability of the oil spray system.

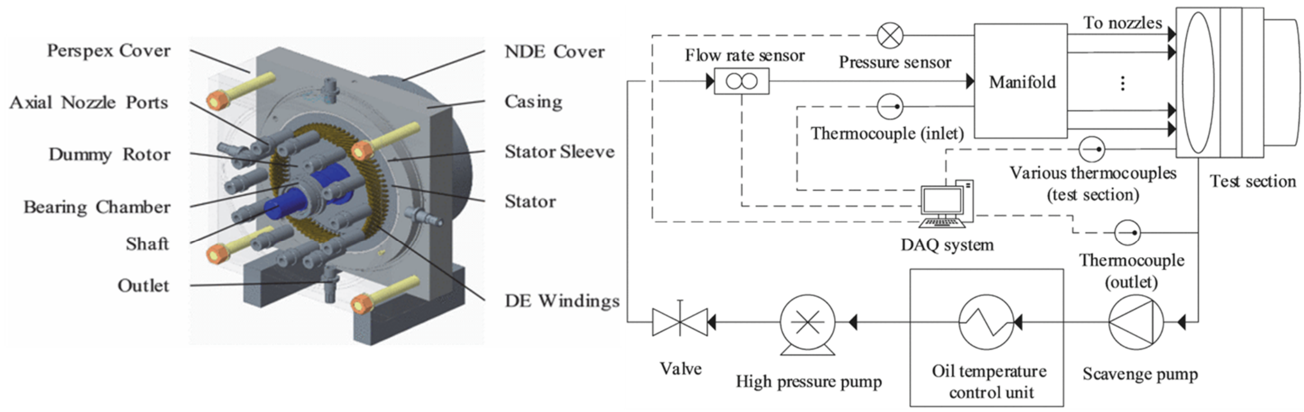

Fig. 29. a) Spray cooling sections of the test rig; b) Fluid system setup [25].

Firstly, they consider the axial spray cooling setup capabilities presented in [25]. As seen in Fig. 30, they installed the 12 nozzles in the clock position system's format on the Perspex cover to provide the axial oil spray. Next, they select three commercial nozzles to consider the different nozzles types; two full cone whirl nozzles with a spray angle of 60° (Nozzle A) and 75° (Nozzle B) and one hollow cone nozzle with a spray angle of 120° (Nozzle C). Finally, they investigate the effects of various nozzle types, nozzle numbers, and fluid flow rates on proposed cooling setups.

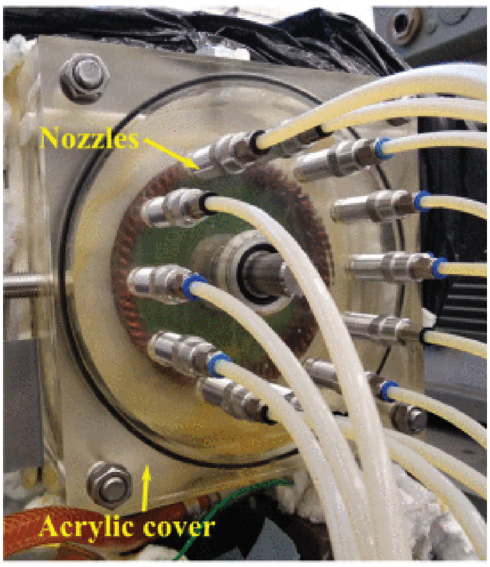

Fig. 30. Axial spray setup with 12 nozzles the clock position system's format [38].

According to the experimental results, their findings are divided into five categories. First, the temperature uniformity is directly proportional to the number of the utilized nozzles and the spray coverage (spray angle and distance); accordingly, the case study with a low number of nozzles and narrow spray angle leads to unwanted hot spots in the system. Further, they observed that the high flow rate nozzle provides a better cooling performance with the same number of nozzles (Fig. 31). As seen in Fig. 31, two whirl full cone nozzles offer better cooling performance than the hollow cone. Moreover, among the setups with the same number of nozzles, the setup with nozzle A provides better cooling performance, and its HTC reaches approximately 3500 (W/m^2/K). However, a hollow cone nozzle can offer better temperature uniformity. Fig. 31 indicates that increasing the number of nozzles may decrease the HTC, if the nozzles' flow rate and nominal outlet velocity are not maintained during the cooling process. Also, in the limited oil flow rate application, they recommended utilizing a higher number of low flow rate nozzles, which leads to higher spray cooling efficiency. Finally, selecting the nozzle mainly depends on cooling equipment, mechanical design, and space from a practical point of view. For instance, when the end space inside the machine's end region is restricted, utilizing several high flow rate nozzles offers an optimum cooling effect.

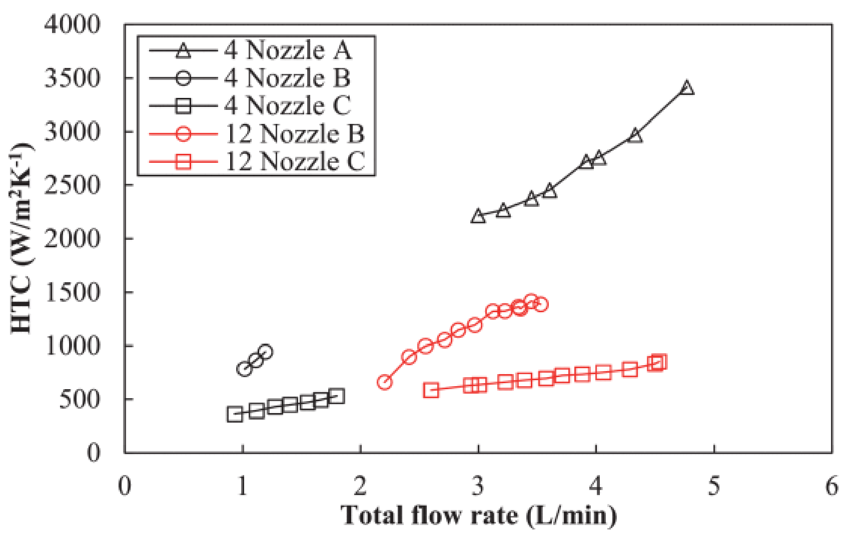

Fig. 31. HTC of various nozzles setups versus total flow rate [25].

The radial spray cooling setup capabilities were also investigated in [89]. As seen in Fig. 32, to investigate the radial oil spray cooling performance, they located the nozzles at 12 o'clock, 3 o'clock, and 9 o'clock positions, and based on their assumptions, due to the gravity effect, the draping oils cool the lower-end windings. After several nozzle tests, they select two types of nozzles: misting nozzle with a spray pattern of a cone-shaped mist and 90° spray angle and a full-cone spray nozzle with the uniform full cone spray pattern and 77° spray angle. Finally, they consider the effects of various nozzle types, the number of nozzles, and fluid flow rates on the proposed cooling setup.

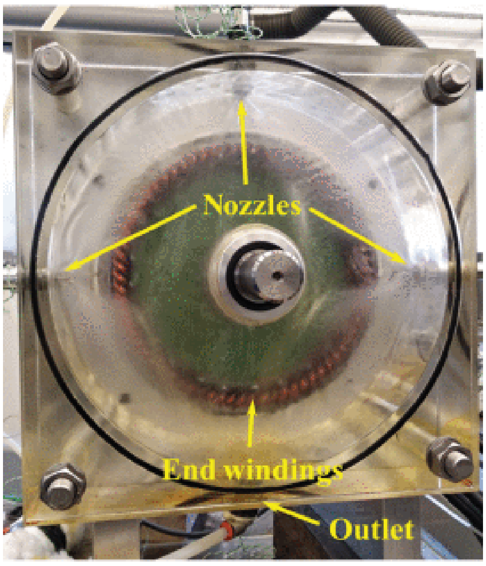

Fig. 32. Axial spray setup with 3 nozzles in the clock position system's format at 12, 3, and 9 o'clock positions [38].

According to their findings and observations, nozzle types play a vital role in temperature uniformity and even temperature distribution in the end-windings region due to their various spray patterns and coverage. Fig. 33 a) and b) show the temperature distributions on the end-windings region of the test rig for misting nozzles and full cone nozzles, respectively. Therefore, the misting nozzles provide a more uniform temperature distribution in the entire end windings than the full cone nozzles. This can happen due to the larger spray angle and coverage of the misting nozzles. Moreover, the lower-end windings have similar temperatures, and the dropping oil films have a considerable cooling impact.

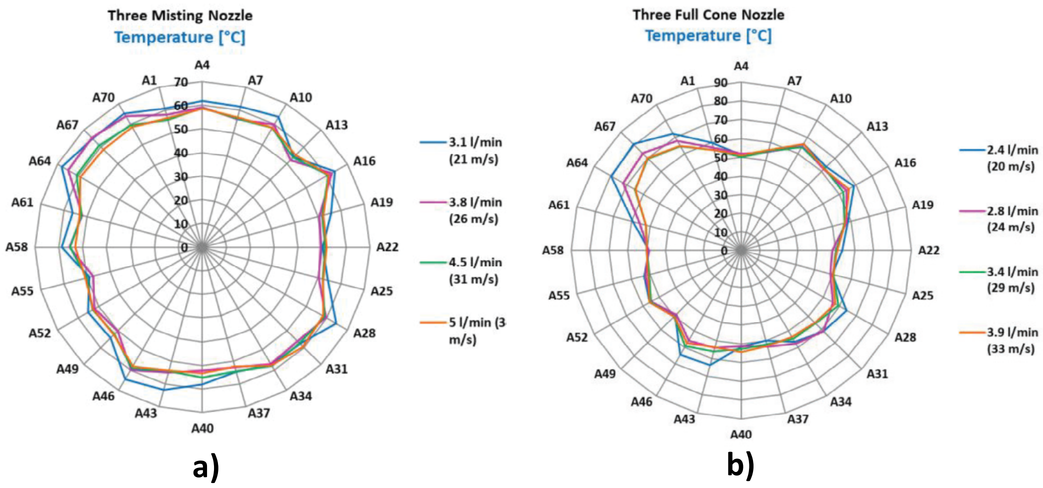

Fig. 33. Temperature distribution on the end windings region: a) three misting nozzles; b) three full cone nozzles [89].

Furthermore, a sufficient number of nozzles directly impact uniform temperature distribution. As seen in Fig. 34, nozzle numbers significantly impact the end windings temperatures. For example, as seen in Fig. 34, a three nozzles setup provides a lower and more even temperature distribution in the end parts; however, the test rig faces higher and uneven temperature distribution in the end regions for a setup with one nozzle setup.

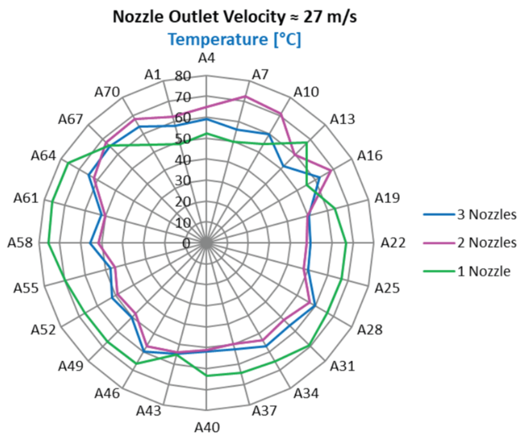

Fig. 34. The impact of nozzle numbers on the temperature distribution of end- winding regions [89].

Table VIII summarizes all the attempts and studies on implementing the spray cooling approach on electrical motors using evaporation coolant and lubricant oils with the information related to injection equipment, coolant, method of analysis, target section, and performances. Accordingly, most studies have relied on experimental approaches, and only a few studies related to the in-wheel motor used the numerical approach. Moreover, a few studies considered the impact of rotor rotation on spray cooling performance. Therefore, it requires more studies and research to find the effect of rotor rotation on the performance of this cooling method.

Table VIII. Summary of spray cooling studies on electrical motors.

Ref	Year	Coolant Type	Nozzle	Cooled section	Rotor rotational speed RPM	Motor Type	Performance	Method
[49]	2009	F-113	Full cone, spray angles of 15~45°	End windings	N/A	Sizeable synchronous generator	A maximum HTC:400000 $W/m^2/K$	Exp.
[48]	2015	R-113	Conical spray nozzle	Stator active part and end windings	0	Sizeable synchronous generator	A maximum of 33% decrease in nodal temperature	Exp.
[79]	2017	ZXB-1	Full cone, Spray angles of 50°;	Copper block	0	Sizeable synchronous generator	A maximum HTC: 5700 $W/m^2/K$	Exp.
[37]	2015	Lubricant oil	Full-cone Flat Jet Dripping Multijets	End windings	0-4600	A middle-range power (40 kW), radial flux machine	A maximum relative global dissipation efficiency is 24.5 W/K	Exp.
[80]	2015	Mercon LV ATF	ATF jets	18, 22, and 26 AWG, samples	0	EV motor	A maximum HTC: 10,000 W/m2/K	Exp.
[82]	2014	N/A	Hollow shaft and holes on the shaft	Coil, stator core, reduction gear, and bearing	4400 and 11000	35-kW in-wheel motor	The maximum temperature of the coil is set below the design point.	Exp. & Num.
[83]	2019	N/A	Hollow shaft and cooling channels	End windings	4400 and 11000	35-kW in-wheel motor	A maximum of 16% decrease in absolute temperature at the coil and a maximum HTC: 10849 $W/m^2/K$	Exp. & Num.
[23]	2019	Lubricant oil	Full-cone & Hollow-cone	End windings	0	A stator with 72 slots with a hairpin winding configuration	A maximum HTC: 3500 $W/m^2/K$	Exp.
[89]	2021	Lubricant oil	Misting & Full-cone	End winding	0	A stator with 72 slots with a hairpin winding configuration	The misting nozzle provides a more uniform temperature distribution than Full-cone	Exp.

IV. Estimation of Heat Transfer Coefficient

The spray cooling approach has been applied over decades in various engineering disciplines due to its high heat transfer capabilities. In parallel, many research studies concentrate on developing the empirical correlation to model and estimate the HTC of spray cooled surfaces for various conditions, including single and two-phase heat transfer regimes.

Table IX presents some of these correlations; accordingly, these empirical correlations have been developed based on the dimensionless number, e.g., Nusselt (Nu), Prandtl (Pr), Reynolds (Re) numbers, and spray Weber number (We). Besides, they are mainly described in the following format:

$\mathrm{Nu} = a\mathrm{Re}^{b}\mathrm{Pr}^{c}$, (11)

where a, b, and c are constants. These constants are mainly defined according to various parameters to make them applicable for various nozzles, coolant, and cooling regimes.

Table IX. Empirical correlations to estimate HTC.

Ref	Coolant Type	Target surface	Injection system	Empirical Correlation
[92]	Water & Oil	Small Heat Sources	Liquid Jet Impingement	$\mathrm{Nu} = \mathrm{Pr}^{0.4}\left[0.785\mathrm{Re}^{0.5}\left(\frac{L}{D}\right)A_r + 0.0257\mathrm{Re}^{0.83}\left(\frac{L}{l}\right)(1 - A_r)\right];$ $A_r = \frac{\pi(1.9d)^2}{L^2};\ l = 0.5(0.5(1+\sqrt{2})L - 3.8d)$
[93]	PF-5052	Small heater	Full-cone nozzle	$\mathrm{Nu} = 4.7\ \mathrm{Re}^{0.61}\mathrm{Pr}^{0.32}$
[94]	Water	Copper cylinder	Full-cone nozzle	$\mathrm{Nu} = 20.344\mathrm{Re}^{0.659}$
[95]	Water	Metallic surfaces	Full-cone nozzle	$\mathrm{Nu} = 2.512\ \mathrm{Re}^{0.76}\mathrm{Pr}^{0.56}$
[96]	R-134a	Flat endplate	Full-cone nozzle	$\mathrm{Nu} = 933\ \mathrm{We}^{0.36}(\frac{D_{32}}{D})^{0.027}$

However, all the above correlations have been established for applications other than electrical machines. Therefore, researchers face several challenges in applying these correlations to electrical machines due to the requirement of knowledge about the mean droplet dimension and the coolant characteristics under a specific temperature. The first issue requires extra equipment, significant investment, and personnel, and the second one needs specific data and parameters, which are mostly not provided by the fluid manufacturers. Ultimately, most of these correlations have been developed for low viscosity coolants, and there is no guarantee that they work for the high viscosity liquids such as lubricant oil.

Therefore, Liu et al. [38] propose a practical and economical approach to estimate the HTC of spray cooling on hairpin windings by establishing the reduced-parameter model. For this purpose, they do not apply the conventional dimensionless correlations and establish the correlation to calculate HTC that encompasses all aspects of spray, flow, fluid, and end winding parameters as follows:

$$h = f(\,spray\ coverage\ and\ patterns, Flow\ , fluid, end\ winding\ dimension) =$$

$$a\left[\frac{\dot{V}\tan\left(\frac{\operatorname{atan}(r_i/D)}{2}\right)}{\pi r_i^2 (D^2+r_i^2)^{0.5}\sin(^{\alpha}/_{2})\tan(^{\alpha}/_{4})}\right]^b p_{in}^c, \quad (12)$$

where $\dot{V}$ is the total flow rate that discharges from the nozzle, r_i is the impingement surface radius, D is the nozzle height, α is the spray angle, p_{in} equals the nozzle's inlet pressure. Moreover, a,b, and c are constants.

Unfortunately, this empirical correlation lacks a rotor rotation effect, and it is mainly developed for the full cone nozzles utilized in their experiments. Therefore, it cannot demonstrate the comprehensive correlation used for all the nozzles and setups.

V. Complementary Discussions

The oil spray cooling of electrical machines seems a promising solution to overcome the challenges and restrictions of conventional thermal management systems. However, it still requires more development and research work in the cooling method, system development, and analysis approaches. Furthermore, the various research works developed so far demonstrate different maturity levels for this thermal management technique. Therefore, this technology is still in progress and in the middle of reaching its desired level.

The cooling method can be considered from two perspectives; oil (coolant) and nozzle (spraying device). Until now, no comprehensive information has been provided for the types of oil and nozzle implemented in EV motors. From oil vision, various research studies used different lubricant oils. However, the cooling system's primary objective for the hybrid vehicle (HV) is to use the available fluid such as air, water, and oil to cool the motor. Table X shows a low-viscosity lubrication oil (LO) utilized by the latest research [25], [38], and one of the lowest viscosity conventional engine oil (ATF 1900) [97], respectively. By simple comparison, the oil as a coolant is utilized in [25], [38] and has a lower viscosity than the engine oil used for HV. As a result, the experiment should focus on the conventional engine oil with a higher viscosity than the oil utilized by the latest research [25], [38].

Table X. Material Properties of the Coolants [25], [97].

Name	**Units**	**Value for LO**	**Value for ATF 1900**
Density at 288.15K (15°C)	kg/L	0.9511	0.845
Kinematic viscosity at 313.15K (40°C)	mm^2/s	12.46	21.0

From a nozzle vision, the research studies used several different experiments by the trial and error technique to find the proper nozzles for their test rig. Also, no information is available for nozzle types, which can provide perfect performance with oil as a high viscosity fluid. Furthermore, in most studies, nozzles are located in the radial (Fig. 35. a) or axial directions (Fig. 35. b). There is no research item to investigate the spraying impact from the nozzle installing inclined condition (Fig. 35. c) for EV motors or finding the proper location for the nozzle to provide perfect spray coverage.

.

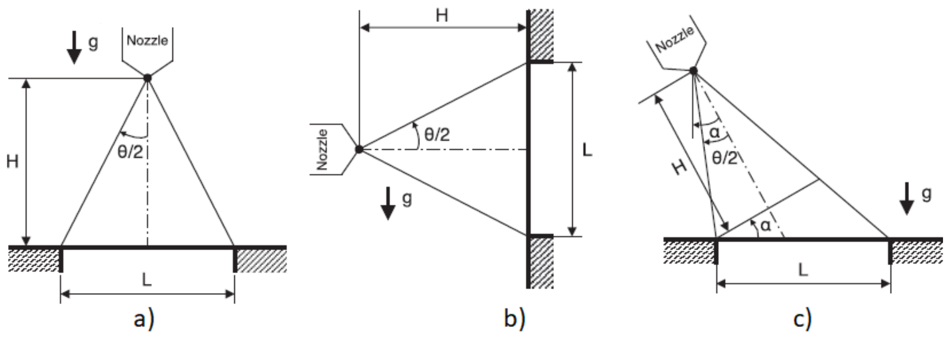

Fig. 35. Different nozzle installment orientations: a) radial, b) axial, c) inclined [69].

Another critical point is implementing the novel additive manufacturing (AM) approaches to design and manufacture proper nozzles for oil spray cooling, i.e., the nozzle can work with high viscosity fluid, which maintains its spray capability. The AM technology allows constructing and locating the nozzle at any angle and challenging area to reach the best cooling efficiency in the restricted area of the motor's end space. General Electric (GE) Aviation uses this technology for 3-D fuel nozzle fabrication to run the liquid fuel and spray it into the airplane engine. The AM technology allows GE Aviation to manufacture the nozzle's entire structure with all the details, such as its twisting and interior chambers geometries in a single part [98]. GE aviation reported that implementing the AM method in the fuel nozzle saves remarkable labor, time, and cost. Moreover, lighter and stronger nozzle fabrication was obtained [98], [99]. However, in contrast with the aviation industry, AM technology's maturity for electrical machines is low, requiring further attempts.

Besides, since vehicles do not always move on a flat surface, and sometimes they move on a slope and downhill, the effect of sloping or inclination on the thermal management system needs to be investigated to provide a more comprehensive view of most of the system positions and its performances.

By taking a closer look at all the research done, the lack of proper investigation of the rotor rotation effect on oil distribution and nozzle performances can be observed. This subject requires more research as oil spray cooling is implemented chiefly in high-speed motor applications.

Ultimately, from the analysis point of view, most of the attempts in oil spray cooling are based on the experimental approach. Therefore, it seems necessary to develop suitable numerical and analytical analysis tools to help designers predict spray cooling performance (for a machine under design) and find correct types, nozzle numbers, and proper mechanical factors such as the system pressure (to boost the coolant).

VI. Conclusions

The paper presented a summary of the spray cooling system and its apparatus for the electric motors. The paper first investigates in detail the evolution of a spray cooling system as a closed-loop cooling technique, with its advantages and drawbacks. Then, according to the latest attempts to replace the lubricant oils as a coolant instead of evaporation one to reduce the system complexity of the spray cooling system, and according to the high viscosity of this liquid rather than refrigerant and water, the paper provides a holistic view of the impact of high viscosity oil on the nozzle performance, such as flow rate, droplet size, and spray coverage. Moreover, it proposes the analytical correlation to recalculate flow rate and nozzle parameters such as droplet size and spray coverage using the lubricant oil characteristics such as SG and viscosity.

The paper also collects all the attempts to implement the spray cooling system for electrical machines with their advantages, drawbacks, and effect of various parameters on the cooling performance and heat removal. Finally, it proposes the correlation to calculate HTC, encompassing all aspects of spray, flow, fluid, and end winding parameters. Overall, the oil spray cooling provides excellent thermal management for the EV motors with a hairpin winding configuration. The authors believe it is only a matter of time to reach the same maturity level as conventional thermal management methods.

REFERENCES

[1] European Commission, “COM(2011) 112 - A Roadmap for moving to a competitive low carbon economy in 2050 — European Environment Agency,” 2011. https://www.eea.europa.eu/policy-documents/com-2011-112-a-roadmap

[2] European Commission, “The roadmap for transforming the EU into a competitive, low-carbon economy by 2050,” pp. 1–4, 2011. Available: https://ec.europa.eu/clima/sites/clima/files/2050_roadmap_en.pdf.

[3] “Annual Progress Reports | Department of Energy.” https://www.energy.gov/eere/vehicles/downloads/electrification-fy2018-annual-progress-report

[4] T. Finken and K. Hameyer, “Design of Electric Motors for Hybrid-and Electric-Vehicle Applications,” 2009. Available: http://134.130.107.200/uploads/bibliotest/2009TFHevEv.pdf.

[5] M. Popescu, J. Goss, D. A. Staton, D. Hawkins, Y. C. Chong, and A. Boglietti, “Electrical Vehicles—Practical Solutions for Power Traction Motor Systems,” *IEEE Trans. Ind. Appl.*, vol. 54, no. 3, pp. 2751–2762, May 2018.

[6] J. Goss, M. Popescu, D. Staton, D. Hawkins, and A. Boglietti, “Electrical vehicles - Practical solutions for power traction drive systems,” in *Proceedings - 2017 IEEE Workshop on Electrical Machines Design, Control and Diagnosis, WEMDCD 2017*, Jun. 2017, pp. 80–88.

[7] T. Davin, J. Pellé, S. Harmand, and R. Yu, “Motor cooling modeling: An inverse method for the identification of convection coefficients,” *J. Therm. Sci. Eng. Appl.*, vol. 9, no. 4, Dec. 2017.

[8] P. O. Gronwald and T. A. Kern, “Traction Motor Cooling Systems: A Literature Review and Comparative Study,” *IEEE Transactions on Transportation Electrification*, vol. 7, no. 4. Institute of Electrical and Electronics Engineers Inc., pp. 2892–2913, Dec. 01, 2021.

[9] M. Popescu, D. Staton, A. Boglietti, A. Cavagnino, D. Hawkins, and J. Goss, “Modern heat extraction systems for electrical machines - A review,” in *Proceedings - 2015 IEEE Workshop on Electrical Machines Design, Control and Diagnosis, WEMDCD 2015*, Aug. 2015, pp. 289–296.

[10] F. Zhang *et al.*, “Back-Iron Extension Thermal Benefits for Electrical Machines with Concentrated Windings,” *IEEE Trans. Ind. Electron.*, vol. 67, no. 3, pp. 1728–1738, Mar. 2020.

[11] S. Nategh *et al.*, “A Review on Different Aspects of Traction Motor Design for Railway Applications,” in *IEEE Transactions on Industry Applications*, May 2020, vol. 56, no. 3, pp. 2148–2157.

[12] P. Shams Ghahfarokhi, A. Kallaste, T. Vaimann, and A. Belahcen, “Thermal Analysis of Totally Enclosed Fan Cooled Synchronous Reluctance Motor-state of art - IEEE Conference Publication,” in *IECON 2019 - 45th Annual Conference of the IEEE Industrial Electronics Society*, 2019, pp. 1–5.

[13] Y. Gai *et al.*, “Cooling of Automotive Traction Motors: Schemes, Examples, and Computation Methods,” *IEEE Trans. Ind. Electron.*, vol. 66, no. 3, pp. 1681–1692, Mar. 2019.

[14] T. Burress and S. Campbell, “Benchmarking EV and HEV power electronics and electric machines,” 2013.

[15] E. Y. C. Chong, “Latest Trends in Cooling of Electric Traction Motors,” in *Motor-desgin limited*, 2018, pp. 1–47.

[16] A. Carriero, M. Locatelli, K. Ramakrishnan, G. Mastinu, and M. Gobbi, “A Review of the State

of the Art of Electric Traction Motors Cooling Techniques," in *SAE Technical Papers*, 2018, vol. 2018-April.

[17] M. Popescu, D. A. Staton, A. Boglietti, A. Cavagnino, D. Hawkins, and J. Goss, "Modern Heat Extraction Systems for Power Traction Machines—A Review," *IEEE Trans. Ind. Appl.*, vol. 52, no. 3, pp. 2167–2175, May 2016.

[18] S. Sano, T. Yashiro, K. Takizawa, and T. Mizutani, "Development of new motor for compact-class hybrid vehicles," *World Electr. Veh. J.*, vol. 8, no. 2, pp. 443–449, Jun.

[19] Lesics, *Tesla Model 3's motor - The Brilliant Engineering behind it*. 2020.

[20] "Technical Feature: The Porsche Taycan." https://newsroom.porsche.com/en_AU/2021/products/technical-feature-the-porsche-taycan-23670.html.

[21] T. N. Lamichhane, L. Sethuraman, A. Dalagan, H. Wang, J. Keller, and M. P. Paranthaman, "Additive manufacturing of soft magnets for electrical machines—a review," *Materials Today Physics*, vol. 15. Elsevier Ltd, p. 100255, Dec. 01, 2020.

[22] P. S. Ghahfarokhi *et al.*, "Opportunities and Challenges of Utilizing Additive Manufacturing Approaches in Thermal Management of Electrical Machines," *IEEE Access*, vol. 9, pp. 36368–36381, 2021.

[23] X. Liu, D. Gerada, Z. Xu, M. Corfield, C. Gerada, and H. Yu, "Effective thermal conductivity calculation and measurement of litz wire based on the porous metal materials structure," *IEEE Trans. Ind. Electron.*, vol. 67, no. 4, pp. 2667–2677.

[24] P. Shams Ghahfarokhi, A. Kallaste, A. Belahcen, and T. Vaimann, "Analytical thermal model and flow network analysis suitable for open self-ventilated machines," *IET Electr. Power Appl.*, Feb. 2020.

[25] C. Liu *et al.*, "Experimental Investigation on Oil Spray Cooling with Hairpin Windings," *IEEE Trans. Ind. Electron.*, vol. 67, no. 9, pp. 7343–7353, Sep. 2020.

[26] P. Lindh *et al.*, “Direct Liquid Cooling Method Verified with an Axial-Flux Permanent-Magnet Traction Machine Prototype,” *IEEE Trans. Ind. Electron.*, vol. 64, no. 8, pp. 6086–6095, Aug. 2017.

[27] P. Lindh, I. Petrov, J. Pyrhonen, E. Scherman, M. Niemela, and P. Immonen, “Direct Liquid Cooling Method Verified with a Permanent-Magnet Traction Motor in a Bus,” *IEEE Trans. Ind. Appl.*, vol. 55, no. 4, pp. 4183–4191, Jul. 2019.

[28] N. A. Rahman, E. Bostanci, and B. Fahimi, “Thermal analysis of switched reluctance motor with direct in-winding cooling system,” Jan. 2017.

[29] E. Nitsche and M. Naderer, “Internally Cooled Hollow Wires Doubling the Power Density of Electric Motors,” *ATZelektronik Worldw.*, vol. 12, no. 3, pp. 42–47, Jun. 2018.

[30] P. Lindh *et al.*, “Performance of a Direct-Liquid-Cooled Motor in an Electric Bus under Different Load Cycles,” *IEEE Access*, vol. 7, pp. 86897–86905, 2019.

[31] Z. Xu *et al.*, “A semi-flooded cooling for a high speed machine: Concept, design and practice of an oil sleeve,” in *Proceedings IECON 2017 - 43rd Annual Conference of the IEEE Industrial Electronics Society*, Dec. 2017, vol. 2017-Janua, pp. 8557–8562.

[32] P. Arumugam *et al.*, “Permanent magnet starter-generator for aircraft application,” in *SAE Technical Papers*, 2014, vol. 2014-Septe, no. September.

[33] A. Tüysüz, F. Meyer, M. Steichen, C. Zwyssig, and J. W. Kolar, “Advanced Cooling Methods for High-Speed Electrical Machines,” *IEEE Trans. Ind. Appl.*, vol. 53, no. 3, pp. 2077–2087, May 2017.

[34] A. Acquaviva, S. Skoog, E. Grunditz, and T. Thiringer, “Electromagnetic and Calorimetric Validation of a Direct Oil Cooled Tooth Coil Winding PM Machine for Traction Application,” *Energies*, vol. 13, no. 13, pp. 33-39, Jun. 2020.

[35] V. Madonna, A. Walker, P. Giangrande, G. Serra, C. Gerada, and M. Galea, “Improved thermal management and analysis for stator end-windings of electrical machines,” *IEEE Trans. Ind.*

Electron., vol. 66, no. 7, pp. 5057–5069, Jul. 2019.

[36] V. Madonna, P. Giangrande, A. Walker, and M. Galea, "On the Effects of Advanced End-Winding Cooling on the Design and Performance of Electrical Machines," in *Proceedings - 2018 23rd International Conference on Electrical Machines, ICEM 2018*, Oct. 2018, pp. 311–317.

[37] T. Davin, J. Pellé, S. Harmand, and R. Yu, "Experimental study of oil cooling systems for electric motors," *Appl. Therm. Eng.*, vol. 75, pp. 1–13, Jan. 2015.

[38] C. Liu *et al.*, "Estimation of Oil Spray Cooling Heat Transfer Coefficients on Hairpin Windings with Reduced-parameter Models," *IEEE Trans. Transp. Electrif.*, pp. 1–1, Oct. 2020.

[39] M. Jaensch, "Cooling Concepts of High-Power Electric Machines," in *Future Powertrain Conference 2019*, Feb. 2019, pp. 1–13.

[40] Y. Gai *et al.*, "Shaft cooling and the influence on the electromagnetic performance of traction motors," Aug. 2017.

[41] "Technology highlight: Audi's internal rotor cooling | Engine + Powertrain Technology International." https://www.enginetechnologyinternational.com/features/technology-highlight-audis-internal-rotor-cooling.html#prettyPhoto.

[42] J. D. Widmer, R. Martin, and M. Kimiabeigi, "Electric vehicle traction motors without rare earth magnets," *Sustain. Mater. Technol.*, vol. 3, pp. 7–13, Apr. 2015.

[43] C. Rhebergen, B. Bilgin, A. Emadi, E. Rowan, and J. Lo, "Enhancement of electric motor thermal management through axial cooling methods: A materials approach," in *2015 IEEE Energy Conversion Congress and Exposition, ECCE 2015*, Oct. 2015, pp. 5682–5688.

[44] W. Sixel, M. Liu, G. Nellis, and B. Sarlioglu, "Ceramic 3D printed direct winding heat exchangers for improving electric machine thermal management," in *2019 IEEE Energy Conversion Congress and Exposition, ECCE 2019*, Sep. 2019, pp. 769–776.

[45] W. Sixel, M. Liu, G. Nellis, and B. Sarlioglu, "Cooling of Windings in Electric Machines via 3-D Printed Heat Exchanger," *IEEE Trans. Ind. Appl.*, vol. 56, no. 5, pp. 4718–4726, Sep. 2020.

[46] R. Thomas, L. Garbuio, L. Gerbaud, and H. Chazal, “Modeling and design analysis of the Tesla Model S induction motor,” in *Proceedings - 2020 International Conference on Electrical Machines, ICEM 2020*, Aug. 2020, pp. 495–501.

[47] Audi, “Audi e-tron cooling concept e-motor (animation) | Video | Audi MediaTV,” 2021. https://www.audi-mediacenter.com/en/audimediatv/video/audi-e-tron-cooling-concept-e-motor-animation-4847.

[48] Z. Li, L. Ruan, and L. Tang, “Heat transfer characteristics of spray evaporative cooling system for large electrical machines,” in *2015 18th International Conference on Electrical Machines and Systems, ICEMS 2015*, Jan. 2016, pp. 1740–1743.

[49] Z. Li, D. Fu, J. Guo, G. Gu, and B. Xiong, “Study on spraying evaporative cooling technology for the large electrical machine,” 2009.

[50] N. Bianchi and G. Berardi, “Analytical Approach to Design Hairpin Windings in High Performance Electric Vehicle Motors,” in *2018 IEEE Energy Conversion Congress and Exposition, ECCE 2018*, Dec. 2018, pp. 4398–4405.

[51] G. Berardi and N. Bianchi, “Design Guideline of an AC Hairpin Winding,” in *Proceedings - 2018 23rd International Conference on Electrical Machines, ICEM 2018*, Oct. 2018, pp. 2444–2450.

[52] G. Volpe, M. Popescu, F. Marignetti, and J. Goss, “AC winding losses in automotive traction e-machines: A new hybrid calculation method,” in *2019 IEEE International Electric Machines and Drives Conference, IEMDC 2019*, May 2019, pp. 2115–2119.

[53] Y. Zhao, D. Li, T. Pei, and R. Qu, “Overview of the rectangular wire windings AC electrical machine,” *CES Trans. Electr. Mach. Syst.*, vol. 3, no. 2, pp. 160–169, Jun. 2019.

[54] J. Kim, “Spray cooling heat transfer: The state of the art,” *Int. J. Heat Fluid Flow*, vol. 28, no. 4, pp. 753–767, Aug. 2007.

[55] D. C. Ludois and I. Brown, “Brushless and permanent magnet free wound field synchronous

motors for EV traction," Pittsburgh, PA, and Morgantown, WV (United States), Mar. 2017.

[56] A. M. El-Refaie *et al.*, "Advanced high-power-density interior permanent magnet motor for traction applications," *IEEE Trans. Ind. Appl.*, vol. 50, no. 5, pp. 3235–3248, Sep. 2014.

[57] I. Mudawar, D. Bharathan, K. Kelly, and S. Narumanchi, "Two-phase spray cooling of hybrid vehicle electronics," *IEEE Trans. Components Packag. Technol.*, vol. 32, no. 2, pp. 501–512, 2009.

[58] I. Mudawar, "Assessment of high-heat-flux thermal management schemes," *IEEE Trans. Components Packag. Technol.*, vol. 24, no. 2, pp. 122–141, Jun. 2001.

[59] B. L. Rowden, D. W. Trowler, and J. C. Balda, "Double sided spray cooled bi-directional power conversion module," in *IEEE Electric Ship Technologies Symposium, ESTS 2009*, 2009, pp. 207–210.

[60] L. J. Turek, D. P. Rini, B. A. Saarloos, and L. C. Chow, "Evaporative spray cooling of power electronics using high temperature coolant," in *2008 11th IEEE Intersociety Conference on Thermal and Thermomechanical Phenomena in Electronic Systems, I-THERM*, 2008, pp. 346–351.

[61] I. Mudawar, D. Bharathan, K. Kelly, and S. Narumanchi, "Two-phase spray cooling of hybrid vehicle electronics," in *2008 11th IEEE Intersociety Conference on Thermal and Thermomechanical Phenomena in Electronic Systems, I-THERM*, 2008, pp. 1210–1221.

[62] H. Bostanci, D. Van Ee, B. A. Saarloos, D. P. Rini, and L. C. Chow, "Thermal management of power inverter modules at high fluxes via two-phase spray cooling," *IEEE Trans. Components, Packag. Manuf. Technol.*, vol. 2, no. 9, pp. 1480–1485, 2012.

[63] "Motor-CAD Software by Motor Design - EMag, Therm and Lab." https://www.motor-design.com/motor-cad-software/.

[64] "BETE Spray Nozzles Company - Spray Nozzle Manufacturers - Spiral Spray Nozzles." https://www.bete.com/.

[65] P. Shams Ghahfarokhi, A. Podgornovs, A. Kallase, T. Vaimann, A. Belahcen, and A. j. marques Cardoso, “Oil Spray Cooling with Hairpin Windings in High- Performance Electric Vehicle Motors,” in *28th International Workshop on Electric Drives: Improving Reliability of Electric Drives (IWED)*, Jan. 2021, pp. 1–5, Accessed: Jan. 29, 2021.

[66] “Spray Nozzles, Fabrications, And Engineered Systems,” BETE, Greenfield, 2020.

[67] A. H. Lefebvre and V. G. McDonell, *Atomization and sprays*, 2nd ed. CRC Press, 2017.

[68] R. J. Schick, “Spray Technology Reference Guide: Understanding Drop Size Preface,” *47th Chem. Process. Ind. Expo.*, p. 6, 1997.

[69] G. Liang and I. Mudawar, “Review of spray cooling – Part 1: Single-phase and nucleate boiling regimes, and critical heat flux,” *International Journal of Heat and Mass Transfer*, vol. 115. Elsevier Ltd, pp. 1174–1205, Dec. 01, 2017.

[70] SNP, “Nozzles for all industries and applications.” https://www.spray-nozzle.co.uk/.

[71] “Nozzles and flushing nozzles - Hansa Engineering - Hansa Engineering.” http://hansa-engineering.se/hansa-dysor-sprayapplikationer/.

[72] T. D. Fansler and S. E. Parrish, “Spray measurement technology: A review,” *Measurement Science and Technology*, vol. 26, no. 1. Institute of Physics Publishing, p. 012002, Jan. 01, 2015.

[73] S. V. Minov, F. Cointault, J. Vangeyte, J. G. Pieters, and D. Nuyttens, “Spray droplet characterization from a single nozzle by high speed image analysis using an in-Focus droplet criterion,” *Sensors (Switzerland)*, vol. 16, no. 2, p. 218, Feb. 2016.

[74] R. A. Mugele and H. D. Evans, “Droplet Size Distribution in Sprays,” *Ind. Eng. Chem.*, vol. 43, no. 6, pp. 1317–1324, Jun. 1951.

[75] E. Babinsky and P. E. Sojka, “Modeling drop size distributions,” *Prog. Energy Combust. Sci.*, vol. 28, no. 4, pp. 303–329, Jan. 2002.

[76] I. Mudawar, “Recent advances in high-flux, two-phase thermal management,” *J. Therm. Sci.*

Eng. Appl., vol. 5, no. 2, May 2013.

[77] K. A. Estes and I. Mudawar, “Comparison of two-phase electronic cooling using free jets and sprays,” *J. Electron. Packag. Trans. ASME*, vol. 117, no. 4, pp. 323–332.

[78] J. X. Wang *et al.*, “Investigation of a spray cooling system with two nozzles for space application,” *Appl. Therm. Eng.*, vol. 89, pp. 115–124, Jun. 2015.

[79] Z. Li, S. Liu, and L. Ruan, “The effect of spray parameter on heat dissipation in spray evaporatvie cooling high power density motors,” Oct. 2017.

[80] K. Bennion and G. Moreno, “Convective heat transfer coefficients of automatic transmission fluid jets with implications for electric machine thermal management,” in *ASME 2015 International Technical Conference and Exhibition on Packaging and Integration of Electronic and Photonic Microsystems, InterPACK 2015, collocated with the ASME 2015 13th International Conference on Nanochannels, Microchannels, and Minichannels*, 2015, vol. 3.

[81] I. D. Chasiotis and Y. L. Karnavas, “Design, Optimization and Modelling of High Power Density Direct-Drive Wheel Motor for Light Hybrid Electric Vehicles,” in *Hybrid Electric Vehicles*, InTech, 2017.

[82] D. H. Lim and S. C. Kim, “Thermal performance of oil spray cooling system for in-wheel motor in electric vehicles,” *Appl. Therm. Eng.*, vol. 63, no. 2, pp. 577–587, Feb. 2014.

[83] D. H. Lim, M. Y. Lee, H. S. Lee, and S. C. Kim, “Performance evaluation of an in-wheel motor cooling system in an electric vehicle/hybrid electric vehicle,” *Energies*, vol. 7, no. 2, pp. 961–971, Feb. 2014.

[84] M. H. Park and S. C. Kim, “Thermal characteristics and effects of oil spray cooling on in-wheel motors in electric vehicles,” *Appl. Therm. Eng.*, vol. 152, pp. 582–593, Apr. 2019.

[85] R. Wang, Y. Chen, D. Feng, X. Huang, and J. Wang, “Development and performance characterization of an electric ground vehicle with independently actuated in-wheel motors,” *J. Power Sources*, vol. 196, no. 8, pp. 3962–3971, Apr. 2011.

[86] A. Saleem, M. Hyeon Park, T. Ambreen, and S. Chul Kim, “Optimization of oil flow distribution inside the in-wheel motor assembly of electric vehicles for improved thermal performance,” *Appl. Therm. Eng.*, vol. 201, p. 117753, Jan. 2022.

[87] P. S. Ghahfarokhi, A. Podgornovs, A. Kallaste, T. Vaimann, A. Belahcen, and A. J. M. Cardoso, “Oil Spray Cooling with Hairpin Windings in High-Performance Electric Vehicle Motors,” Jan. 2021.

[88] S. Xue, “Maximising E-Machine Efficiency with Hairpin Windings,” Wrexham, 2021.

[89] Y. C. Chong *et al.*, “Experimental characterisation of radial oil spray cooling on a stator with hairpin windings,” in *IET Conference Publications*, 2020, vol. 2020, no. CP766, pp. 879–884.

[90] F. Zhang *et al.*, “A Thermal Modeling Approach and Experimental Validation for an Oil Spray-Cooled Hairpin Winding Machine,” *IEEE Trans. Transp. Electrif.*, vol. 7, no. 4, pp. 2914–2926, Dec. 2021.

[91] C. Liu *et al.*, “Model Calibration of Oil Jet and Oil Spray Cooling in Electrical Machines with Hairpin Windings,” Nov. 2021, pp. 3813–3820.

[92] D. J. Womac, S. Ramadhyani, and F. P. Incropera, “Correlating equations for impingement cooling of small heat sources with single circular liquid jets,” *J. Heat Transfer*, vol. 115, no. 1, pp. 106–115, Feb. 1993.

[93] J. R. Rybicki and I. Mudawar, “Single-phase and two-phase cooling characteristics of upward-facing and downward-facing sprays,” *Int. J. Heat Mass Transf.*, vol. 49, no. 1–2, pp. 5–16, Jan. 2006.

[94] N. Karwa, S. R. Kale, and P. M. V. Subbarao, “Experimental study of non-boiling heat transfer from a horizontal surface by water sprays,” *Exp. Therm. Fluid Sci.*, vol. 32, no. 2, pp. 571–579, Nov. 2007.

[95] I. Mudawar and W. S. Valentine, “Determination of the local quench curve for spray-cooled metallic surfaces,” *J. Heat Treat.*, vol. 7, no. 2, pp. 107–121, Sep. 1989.

[96] S. S. Hsieh and C. H. Tien, “R-134a spray dynamics and impingement cooling in the non-boiling regime,” *Int. J. Heat Mass Transf.*, vol. 50, no. 3–4, pp. 502–512, Feb. 2007.

[97] “LIQUI MOLY Top Tec ATF 1900.” https://pim.liqui-moly.de/pidoc/P000238/3648-TopTecATF1900-30.0-en.pdf.

[98] C. Scott, “GE Aviation 3D Prints 30,000th Metal 3D Printed Fuel Nozzle at Auburn, Alabama Plant | 3DPrint.com | The Voice of 3D Printing / Additive Manufacturing,” 2018.

[99] D. Sher, “GE Aviation already 3D printed 30,000 fuel nozzles for its LEAP engine,” *3D Printing Media Network*, 2018.